# SIGNIFICANCE OF MICROBIAL BINDING IN THE FORMATION AND STABILIZATION OF CARBONATE FOREREEF SLOPE DEPOSITS

By

ALEJANDRA SANTIAGO TORRES

Bachelor of Arts and Sciences in Geology

University of Puerto Rico

Mayagüez, Puerto Rico

2017

Submitted to the Faculty of the
Graduate College of the
Oklahoma State University
in partial fulfillment of
the requirements for
the Degree of
MASTER OF SCIENCE
July, 2019

SIGNIFICANCE OF MICROBIAL BINDING IN THE

FORMATION AND STABILIZATION OF

CARBONATE FOREREEF SLOPE DEPOSITS

Thesis Approved:

Dr. G. Michael Grammer

Thesis Adviser

Dr. Jay Gregg

Dr. Dennis Prezbindowski

ACKNOWLEDGEMENTS

First and foremost, I would like to sincerely thank my advisor, Dr. Michael Grammer. If it wasn't for his constant support and advice I would have not been able to accomplish anything. I am eternally grateful of him taking me in as a student and for supporting me throughout the many challenges that these two years in Oklahoma have brought me. I am lucky to have such a supportive advisor and friend. I would also like to thank my committee members Dr. Jay Gregg and Dr. Dennis Prezbindowski for their support and genuine excitement over my project. Having a committee that was so curious with my work pushed me to do my best. I would also like to thank the Boone Pickens School of Geology for giving me the opportunity to learn in a challenging and supportive graduate school environment. Specifically, I would like to thank Dr. Laó Dávila because without him I would not be here. I learned about OSU through him in my internship to Malawi and I am sure that he must have said great things to Dr. Grammer about me so to him I am grateful.

I would also like to thank my lab mates who have been a source of constant laughs, inside jokes, shoulders to cry on, and amazing academic feedback. Words can't even begin to explain how much it meant to me to have them here helping me through every step. A special mention goes to Elizabeth Elium who has been instrumental in these last days of my Master's. I truly appreciate her advice and I am happy to call her a friend. I would also like to thank Ibukun Bode for being my go to person when I moved from Puerto Rico and for always being there when I needed her. Both of these ladies are my inspiration and I hope to one day be as amazing as them

I would also like to thank My Tribe: Estefanny Dávalos, Gokce Astekin, Seyi Sholanke, and Andrew Bean. Being far from home is something that we all can relate to and I am glad that I found this amazing group of humans. Our bond is one of the strongest things I've ever experienced. They have become my family away from home and my rock this past year. I hope we have many years of friendship left and a few weddings to celebrate soon!

Lastly, I would like to thank my family back home. My parents, Leticia and Raul, who have had the patience to deal with me through these two years and still manage to miss me every day. Words will always fail to tell them how much they mean to me but I will try for the rest of my life. I would also like to thank my older sister, Verónica, for being the one I knew I could call crying at 10:00pm and for being my source of hope during the tough times we faced during Hurricane Maria. I would also like to thank my baby nephew, Sebastián, who I hope one day will read this and think his Auntie was cool. ¡Los amo!

Name: ALEJANDRA SANTIAGO TORRES

Date of Degree: July, 2019

Title of Study: SIGNIFICANCE OF MICROBIAL BINDING IN THE FORMATION AND STABILIZATION OF CARBONATE FOREREEF SLOPE DEPOSITS

Major Field: GEOLOGY

Abstract:

The geometry of carbonate slope deposits has been described as being the result of platform height and the volume of sediment transported from the platform, sediment texture and response to shear strengths, the balance between erosion and deposition, early lithification by abiotic marine cements, and in situ carbonate production and stabilization by microbial carbonates. Recent studies of modern examples of the Holocene in the Tongue of the Ocean (TOTO) in the Bahamas and the Miocene of the Cariatiz platform in SE Spain propose that the influence of these microbial carbonates, specifically microbial binding, is a significant early-stage slope-stabilizing factor in steep (35-45°) carbonate slopes. This microbial binding prevents slope failure by providing an early-stage lithification and preserves steep depositional slopes, which sometimes reach the angles of repose.

Although the effect of microbial binding in slope stabilization and lithification is well documented in Cenozoic examples of steep carbonate slopes, its significance and relationship with syndepositional abiotic marine cements in Paleozoic reef systems and steep carbonate slope deposits has not yet been fully determined or understood. Given the growing number of studies supporting the role of microbes in the precipitation of micrite, as well as binding and trapping, this study aims to describe microbial fabrics that may indicate in situ microbial production and syndepositional lithification. Results from this project will provide insights into the relationship between microbial binding and syndepositional abiotic marine cements in ancient reef systems in order to explain the early lithification and evolution of steep carbonate slopes such as forereef slopes, and further develop the fundamentals of sedimentology and diagenesis of Silurian (Niagaran) reefs in and around the Michigan Basin.

TABLE OF CONTENTS

Chapter Page

LIST OF TABLES

Table Page

LIST OF FIGURES

Fig. Page

# CHAPTER I

## INTRODUCTION

The geometry of carbonate slope deposits has been described as being the result of platform height and the volume of sediment transported from the platform (Schlager 1981), sediment texture and response to shear strengths (Kenter et al. 2005), the balance between erosion and deposition (Schlager and Camber, 1986), early lithification by abiotic marine cements (Grammer et al. 1993a; Grammer et al. 1993b), and *in situ* carbonate production and stabilization by microbial carbonates (Della Porta et al. 2003; Kirkland et al. 1998). Recent studies in modern examples of the Holocene of the Tongue of the Ocean (TOTO) in the Bahamas and the Miocene of the Cariatiz platform in SE Spain propose that the influence of these microbial carbonates, specifically microbial binding, is a significant early-stage slope-stabilizing factor in steep (35-45°) carbonate slopes (Reolid et al. 2017, 2014). This microbial binding prevents slope failure by providing early-stage lithification and aids in the preservation of steep depositional slopes, stabilized at or slightly above angles of repose (Reolid et al. 2017). Other examples of early microbial binding include a high-rising carbonate platform of Late Carboniferous age which has a microbial boundstone-dominated slope with dips varying from 20-45° (Della Porta et al. 2003).

These steep slopes are attributed to *in situ* production of microbial carbonates and rapid abiotic marine cementation (Della Porta et al. 2003). Webb (1996) previously discussed the importance of microbial carbonates and biologically induced cementation to the contribution of both the volume of the reef framework and rigidity throughout the Phanerozoic and concluded that it has equaled or exceeded the contributions of skeletal metazoans. Webb (1996) also indicates that biological carbonate precipitation allows organisms that would ordinarily not be considered reef constructors to create a rigid framework. An example of this is observed in a Late Miocene *Halimeda* algal-microbial reef where early lithification by micritic carbonates and abiotic marine cements stabilized algal plates that otherwise could have been readily transported by binding them close to their sites of growth, enhancing reef accretion and relief (Martin et al. 1997). Moore (2001) suggested that pelleted, microbial crusts described in numerous examples from mud mounds and reefs, are the most important type of ancient reef-related cements and that it occurs in reefs throughout the Phanerozoic in combination with aragonitic botryoidal cements and calcitic radiaxial cements.

Although the effect of microbial binding in slope stabilization and lithification is well documented in Cenozoic examples of steep carbonate slopes, its significance and relationship with syndepositional abiotic marine cements in Paleozoic reef systems and steep carbonate slope deposits has not yet been fully determined or understood. Given the growing number of studies supporting the role of microbes in the precipitation of micrite, as well as binding and trapping, this study aims to describe microbial fabrics that may indicate *in situ* microbial production and syndepositional lithification.

Results from this project will provide insights into the relationship between microbial binding and syndepositional abiotic marine cements in ancient reef systems in order to explain the early lithification and evolution of steep carbonate slopes such as forereef slopes, and further develop the fundamentals of sedimentology and diagenesis of Silurian (Niagaran) reefs in and around the Michigan Basin.

The Late Silurian (Cayugan) reef complex exposed at the Pipe Creek Jr. Quarry (IN) provides an excellent opportunity to evaluate the contribution of microbial binding and its relationship with syndepositional abiotic marine cements in steep forereef slope deposits. These deposits are characterized by steeply dipping beds (35-45°) consisting of crinoidal grainstones with abundant syndepositional abiotic marine cement as well as marine micritic cements (Simo and Lehmann, 2000). This study uses an integrated approach involving petrographic analysis, Cathodoluminescence Microscopy (CL), and Scanning Electron Microscopy (SEM) of forereef slope samples to:

(1) Document the presence of microbial binding in the steep Silurian forereef slope deposits at the Pipe Creek Jr. quarry;
(2) Evaluate the contribution of microbial binding to the stabilization and lithification of these deposits;
(3) Determine the paragenetic relationship between microbial binding and abiotic marine cements, and;
(4) Evaluate whether there is a windward vs. leeward orientation of the reef complex based on the relative amounts and distribution of microbial binding and syndepositional abiotic marine cements in the different locations (west, east, and south) of the quarry.

# CHAPTER II

## GEOLOGIC BACKGROUND, STUDY AREA, AND METHODS

### *Microbial carbonates*

Microbial carbonates are produced by benthic microbial communities, which include bacteria, cyanobacteria, and algae (Riding, 1991). There are three main processes involved in the formation of microbial carbonates: 1) trapping or agglutination of particles, 2) biomineralization of organic tissues, and 3) mineralization (Riding, 1991). Other processes include microbially mediated organomineralization which involves mineral precipitation within non-living organic substrates (Trichet and Défarge, 1995; Diaz et al. 2017). In general, microbial carbonates can be classified into five main categories: 1) stromatolites-, laminated microbial deposits, 2) dendrolites-, dendritic microbial deposits, 3) thrombolites-, clotted microbial deposits, 4) travertine-, layered microbial deposits with a dendritic macrofabric, and 5) cryptic microbial carbonates (Riding, 1991). Cryptic microbial carbonates are an important component of reefal facies throughout the Phanerozoic. Unlike the other categories of microbial carbonates, cryptic microbial carbonates lack distinctive macrofabrics but typically possess micritic, clotted or peloidal microfabrics which may also contain traces of bacterial filaments (Riding, 1991).

*Microbial Carbonates in Reefs and Steep Carbonate Slopes*

The presence of microbial carbonates and biologically induced cements along with abiotic marine cements has been well documented in reefs throughout the Phanerozoic (Webb, 1996). Nevertheless, the role of these diagenetic processes in reef framework and volume is still debated. Some suggest that biologically induced microbialite and cements may be equal or more important to reef framework accretion than carbonate secreted enzymatically by skeletal organisms (Webb, 1996). Early Ordovician reefs have been documented where large microbialite and sponge dominated pinnacle reefs, which lacked abundant skeletal metazoans, apparently still flourished (Webb, 1996). Silurian reefs like the Pipe Creek Jr. reef complex and those described from the nearby Michigan Basin (Shaver and Sunderman, 1989; Trout et al. 2017; Wold and Grammer, 2017; Ritter and Grammer, 2017) are composed primarily of stromatoporoids, corals and bryozoans, with abundant syndepositional cements (Webb, 1996; Simo and Lehmann, 2000; Ritter and Grammer, 2017) and a significant portion of microbialite and calcimicrobes (Webb, 1996). In Devonian shallow-water reefs like the Iberg reef complex of Germany, the primary reef builders are stromatoporoids and corals, but calcimicrobes and synsedimentary cements play an important role particularly in the forereef facies of the windward margin of the reef (Webb, 1996), similar to what was also described by Trout and Grammer (2017) for Silurian reefs in the Michigan Basin. Middle Triassic examples include the Latemar reef buildup of the central Dolomites (northern Italy) which have steeply dipping foreslope clinoforms that consist of *Tubiphytes*-rich boundstone facies (Harris, 1993). This boundstone facies consists of skeletal remains with associated biotic crusts, internal sediments and syndepositional cements (Harris, 1993).The biotic crusts

exhibit gravity-defying geometries and micritic laminae (Harris, 1993). A modern example in the Red Sea of Sudan has been documented where laminar micrite crusts form on horizontal ledges along steep forereef slopes of atolls and barrier reefs (Brachert and Dullo, 1991). These laminar micrite crusts appear to be organically induced and are associated with branched micritic tubes related to filamentous algae, bacteria or fungi (Brachert and Dullo, 1991).

In steeply dipping (30-45°) carbonate slope deposits, microbial influence has been shown to be a factor in the stabilization and lithification of these deposits. Examples of carbonate slopes characterized by microbial binding include recent studies on steep carbonate slopes of the Holocene of the Tongue of the Ocean (TOTO) of the Bahamas and the Miocene Cariatiz Platform in SE Spain (Reolid et al. 2014, 2017). Other examples include the Miocene of the Gulf of Suez (Haddad et al. 1984) and Sorbas Basin in Spain (Martin et al. 1997), as well as the Jurassic of Morocco (Della Porta et al. 2013), and the Cretaceous of Mexico (Enos 1977). In these carbonate slope deposits, microbial influence has been described as including clotted peloidal micrite, peloidal aggregates, and automicrite (Keim and Schlager, 1999). It can also be seen as distinct microfabrics indicating microbial binding which include: (1) clotted micritic patches that locally connect bioclasts; (2) dense micritic masses; (3) trapping and binding structures; as well as 4) peloidal textures (Reolid et al. 2017). These microfabrics (1-4) were the dominant criteria used to describe microbial binding in the Silurian forereef slope deposits of the Pipe Creek Jr. reef complex.

*Study Area*

Deposition of the Late Silurian (Cayugan) Pipe Creek Jr. reef complex occurred on

the Wabash Platform in a tropical (to subtropical) setting in normal marine water (Simo and Lehmann, 2000). This platform extends from eastern Iowa to western Ohio (200,000 $km^2$) and is bounded to the southwest by the proto-Illinois basin (previously termed Vincennes Basin in the Siluro-Devonian; Spengler and Read, 2010), to the north by the Michigan Basin, and to the east by the Appalachian Basin (Fig. 1A). The Wabash Platform has been interpreted as a carbonate ramp (overall slope regionally of less than 1°) that lacks a notable shelf break, and is characterized by discontinuous reef trends (Fig. 1B) (Spengler and Read, 2010).

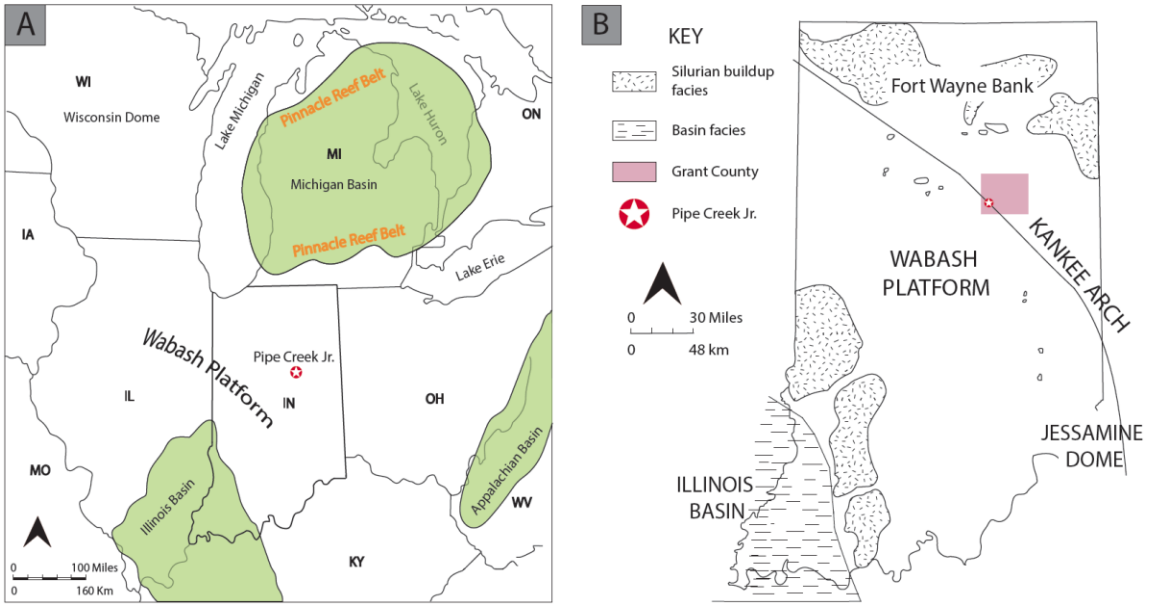


Figure 1: Silurian paleogeographic reconstruction showing nearby basins and main structural features. A) Silurian paleogeography showing the approximate location of the Wabash Platform, adjacent basins, pinnacle reef belts and the current location of Pipe Creek Jr. Quarry (Modified from Trout et al., 2017); B) Close up view of Indiana showing the Wabash Platform, Fort Wayne Bank, Kankee Arch, Jessamine Dome, and the location of Grant County as well as the Pipe Creek Jr. Quarry (Modified from Spengler and Read, 2010).

The reef and associated flank beds exposed at the Pipe Creek Jr. Quarry are located in North Central Indiana in Grant County (Fig. 1B). This quarry has approximately 5 km of exposure with quarry walls ranging in height from 15-30 m. Pipe Creek Jr. Quarry is

currently an active quarry that supplies high calcium limestone for a range of purposes including various construction uses and as an additive to animal feed. The quarry can be broken into three active pits: West, East, and South (Fig. 2).

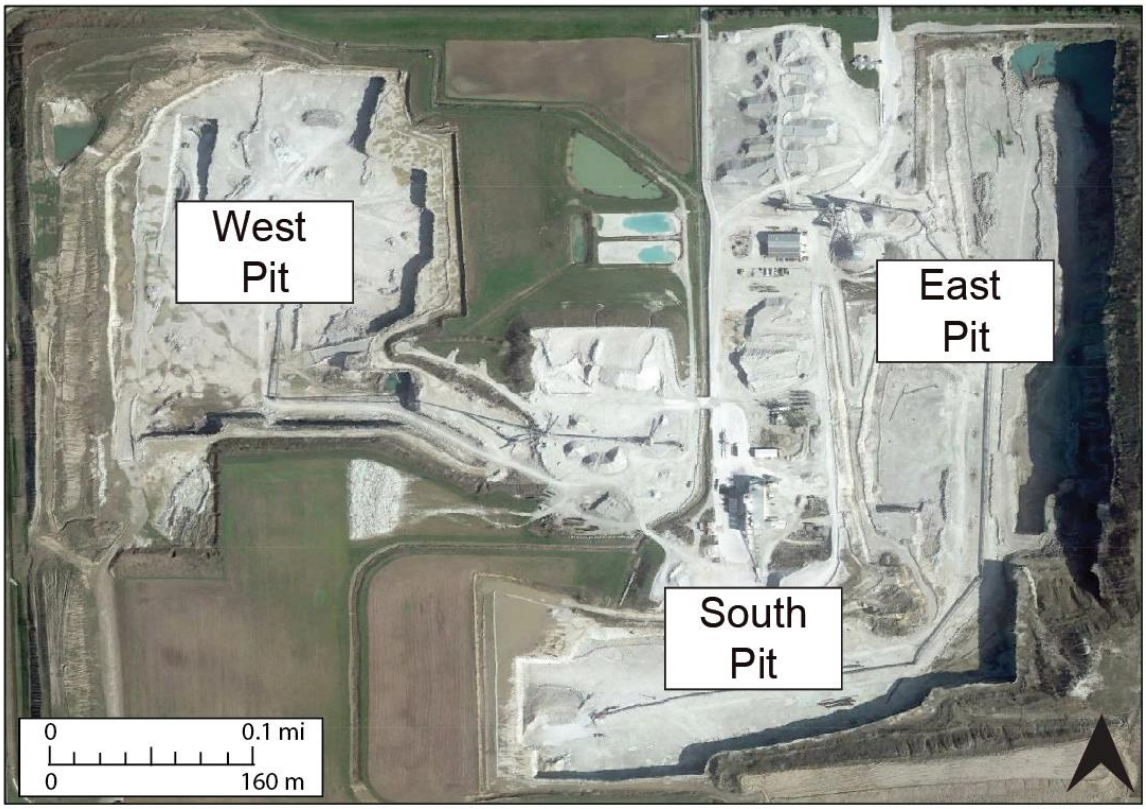


Figure 2: Aerial image of the active limestone quarry Pipe Creek Jr. Quarry. The quarry can be divided into three active pits which are labeled West, East, and South Pits. Arrow points North. (Source: Google Earth).

Reef growth began in a period of high relative sea level and terminated in the Middle to Late Ludlovian when relative sea level was low and evaporite deposition dominated (Simo and Lehmann, 2000). Reef truncation was a result of the sub-Kaskaskia unconformity which is characterized at Pipe Creek Jr. Quarry by caves and fractures that crosscut bedding (Simo and Lehmann, 2000). This reef complex has an inferred circular geometry, with a minimum thickness of 48 m, and a minimum width of 1.4 km (Simo and Lehmann, 2000). The original height of the reef is postulated to be 35-200 m (Fleming et al. 2018), but an exact thickness is uncertain due to post-depositional erosion

of the reef. The reef complex is described as a coral–stromatoporoid and micrite mound with steeply dipping forereef slope deposits (Simo and Lehmann, 2000). These forereef slope deposits are volumetrically significant, and in contrast to most Silurian reefs in the area which have been extensively dolomitized (Simo and Lehmann, 2000), are preserved largely as limestone. This lack of dolomitization is reported to be partly due to syndepositional abiotic marine cementation (Fig. 3) and the resulting reduction in porosity and permeability (Shaver and Sunderman, 1989). Later stages of cementation such as shallow-phreatic (meteoric) calcite cements and postdepositional burial cements (also calcite) further occlude remaining porosity in these deposits (Simo and Lehmann, 2000).

Three depositional facies are described in the reef complex based on their geometries and faunal distribution (Simo and Lehmann, 2000). These include 1) reef flank facies, 2) transition from reef-flank to inter-reef facies, and 3) inter-reef facies (Simo and Lehmann, 2000). The forereef slopes exposed in the quarry consist of the reef-flank facies which are distinguished by their tabular to wedge-shaped bed geometries with thicknesses from 15 cm to 100 cm and depositional dips ranging 35° to 45° (Simo and Lehmann, 2000). This reef complex has been the focus of previous studies and summaries of Niagaran reefs by Sunderman and Mathews (1975), Suchomel (1975), Beerbower (1977), Lehmann (1978), Shaver and Sunderman (1989), Devaney et al. (1986), Lehmann and Simo (1988), Frank et al. (1993), and Simo and Lehmann (2000).

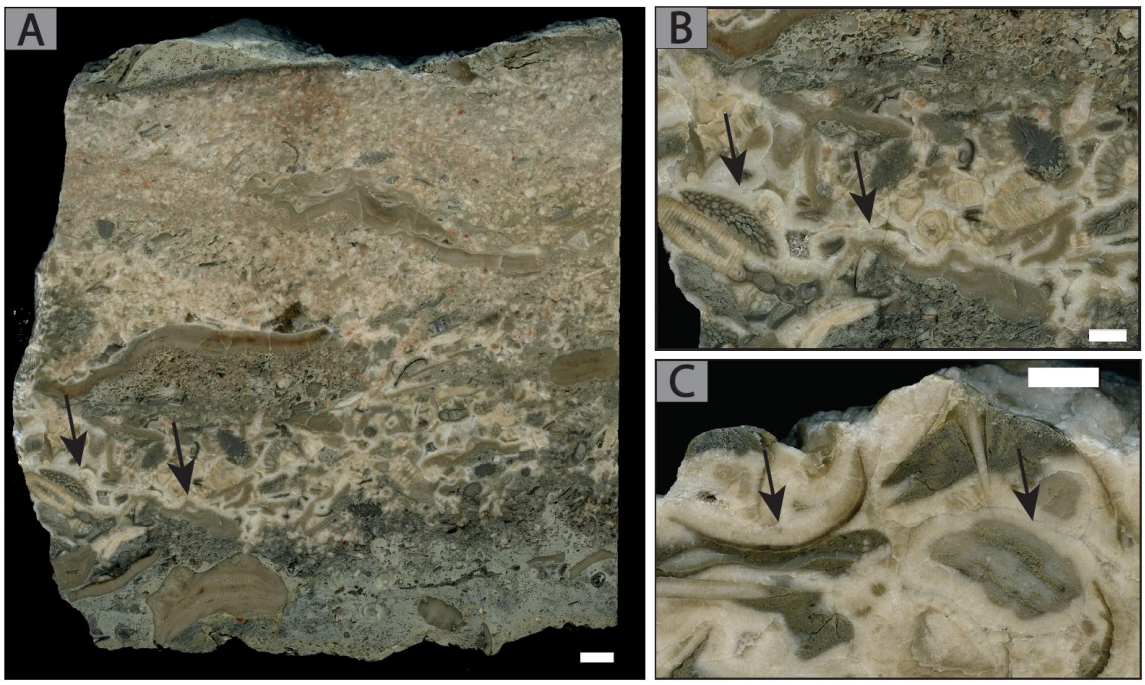

Figure 3: Pervasive abiotic marine cementation in the forereef slope deposits exposed at the Pipe Creek Jr. Quarry: A) Slabbed sample that shows a transition in facies from the bottom to the top of the sample as well as a pervasively cemented section with isopachous cements (black arrows) (Scale bar: 1 cm); B) Close-up of white to light-gray isopachous cements (Scale bar: 1 cm); C) Hand samples show isopachous cements that can reach up to a few centimeters in thickness (Scale bar: 1 cm).

*Methods*

Pipe Creek Jr. Quarry is an active quarry, therefore strict safety regulations limit sampling in zones with a close proximity to the quarry walls. For this reason, samples from the quarry can only be taken from rubble on the quarry floor that resulted from blasting or from cores taken by Irving Material, Inc. (IMI). Samples selected for this study were based on the presence of cement morphologies visible in hand specimen that are typically found in reef systems (Flügel, 2004), as well as their location within the West, East, and South Pits of the quarry to determine a windward/leeward orientation of the reef. Samples collected for the purpose of this study include 33 2.5 cm diameter plugs as well as 9 slabbed samples. Physical characteristics such as the color of these cements

were defined through the use of the Munsell Color System (Goddard et al. 1970). Petrographic analysis of thin sections (n=113) was performed using a Leica DM 2700P optical microscope. Facies were described using the Dunham (1962) classification scheme for carbonate rocks, and microfabrics of microbial binding were identified using fabrics presented in Reolid et al. (2017). Bacelle and Bosellini (1965) visual estimation charts were used to calculate the relative percentage of cements seen through petrography from samples collected from each of the pits (West, East, and South). Selected petrographic thin sections (n=5) were analyzed under Cathodoluminescence excitation (CL) using a CITL MK5-1 cold cathode optical cathodoluminescence apparatus mounted on an Olympus BX51 polarizing microscope. Photomicrographs of each thin section were taken using a "Q-Color 3" cooled (low light) 5-megapixel digital camera for further evaluation. This was done to evaluate multiple episodes of abiotic cementation (syndepositional and post depositional) and to determine a general cement paragenesis to compare with previous work (Simo and Lehmann, 2000). Cement samples from slabbed hand samples were drilled using a microdrill and were analyzed for stable isotopes of carbon ($\delta^{13}C$) and oxygen ($\delta^{18}O$) isotope composition. Carbon and oxygen isotope analyses for all samples were run at the Stable Isotope Laboratory at the University of Miami's Rosenstiel School of Marine and Atmospheric Science. In addition to a petrographic description of the microfabrics indicative of microbial binding, micro- to nano-scale microbial characteristics were further investigated using an FEI Quanta 600F field emission environmental scanning electron microscope (ESEM). Selected samples (n= 11) showing microfabrics indicative of microbial binding were prepared using a JEOL IB-19500CP cross section ion beam polisher to enable high magnification 2D images of the samples with further ESEM analysis.

# CHAPTER III

## RESULTS AND INTERPRETATIONS

### *Facies*

The forereef slope deposits of the Pipe Creek Jr. reef complex consist of two main facies, Facies 1 and 2. Facies 1 is composed of coarse grainstones to packstones with skeletal crinoid, bryozoan, stromatoporoids, and coral fragments, as well as abundant syndepositional abiotic marine cements (see Tables 1-5). This syndepositional abiotic marine cements are preceded by microbial micrite and postdated by postdepositional abiotic cements (Fig. 4). Facies 2 is composed of stromatactis mudstones to wackestones. In Facies 1, most of the bioclasts are observed in a matrix of micrite with relatively abundant crystalline cements. Most of the samples discussed in this work are from Facies 1.

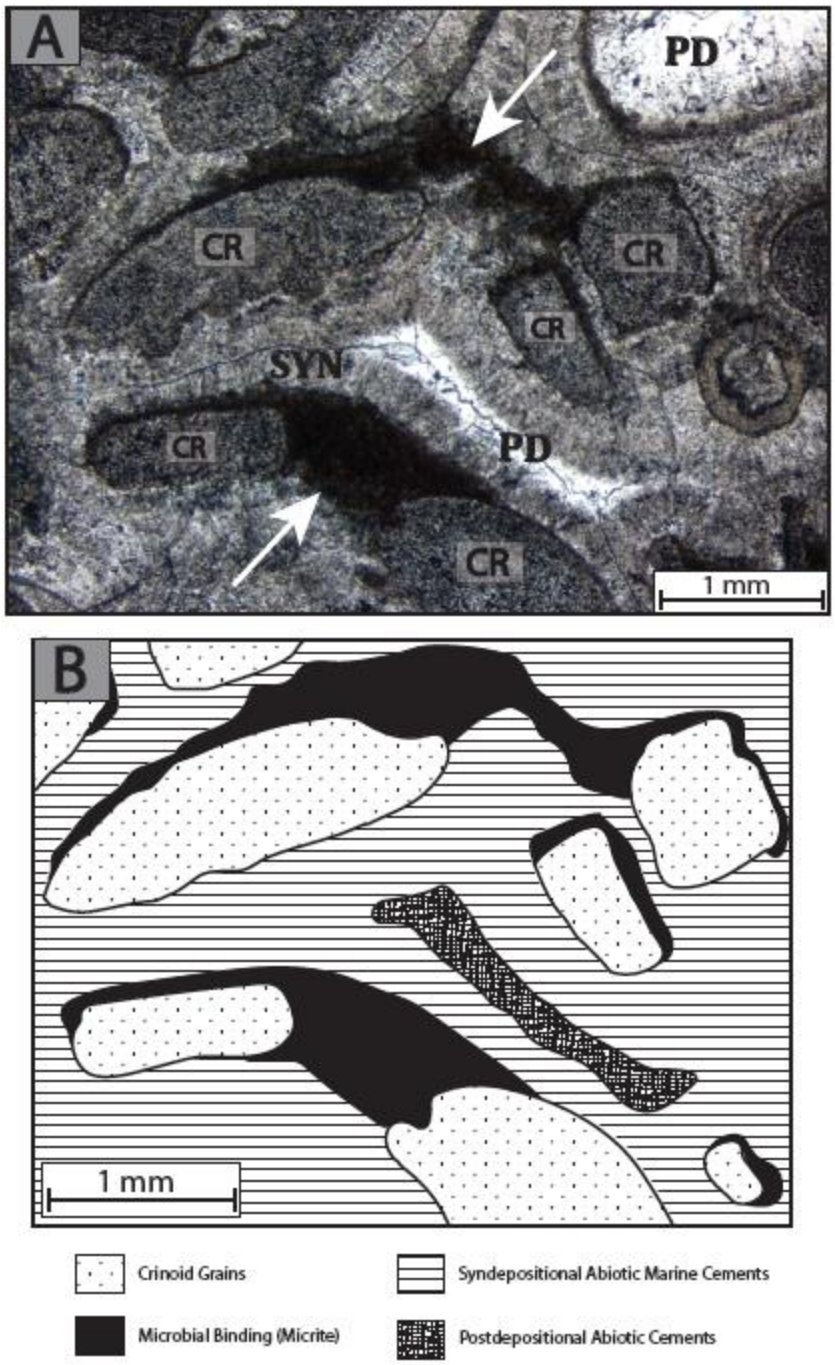


Figure 4: Photomicrograph of Facies 1 of the forereef slope deposits and corresponding schematic diagram showing a paragenetic relationship between microbial micrite, syndepositional abiotic marine cements, and postdepositional abiotic cements. A) Micrite bridges (white arrows) can be seen connecting crinoid grains (CR) and surrounded by syndepositional cements (SYN). Postdepositional cements (PD) can be seen occluding remaining porosity. B) Schematic diagram showing paragenetic relationship between microbial micrite, syndepositional abiotic marine cements, and postdepositional abiotic cements.

### *I. Micritic Matrix and Microbial Binding*

The micritic component of the matrix varies from micrite with a depositional origin often termed ‘sea floor micrite’ (Reid et al. 1990) to a micrite cement which exhibits multiple microfabrics. Some of these fabrics include dense to layered clotted micrite (Fig. 5A) and locally, this micrite also appears as peloidal (Riding, 2000 and Flügel, 2004) and presents some dendritic structures (Fig. 5B). In many cases the dense to clotted micrite creates a bridge-like structure that locally connects crinoid and other skeletal fragments (Fig. 5C). Other fabrics include trapping and binding micrite and micritic crusts that show preferential development on the upper side (top) of the bioclasts based on nearby geopetal structures (Fig. 5D).

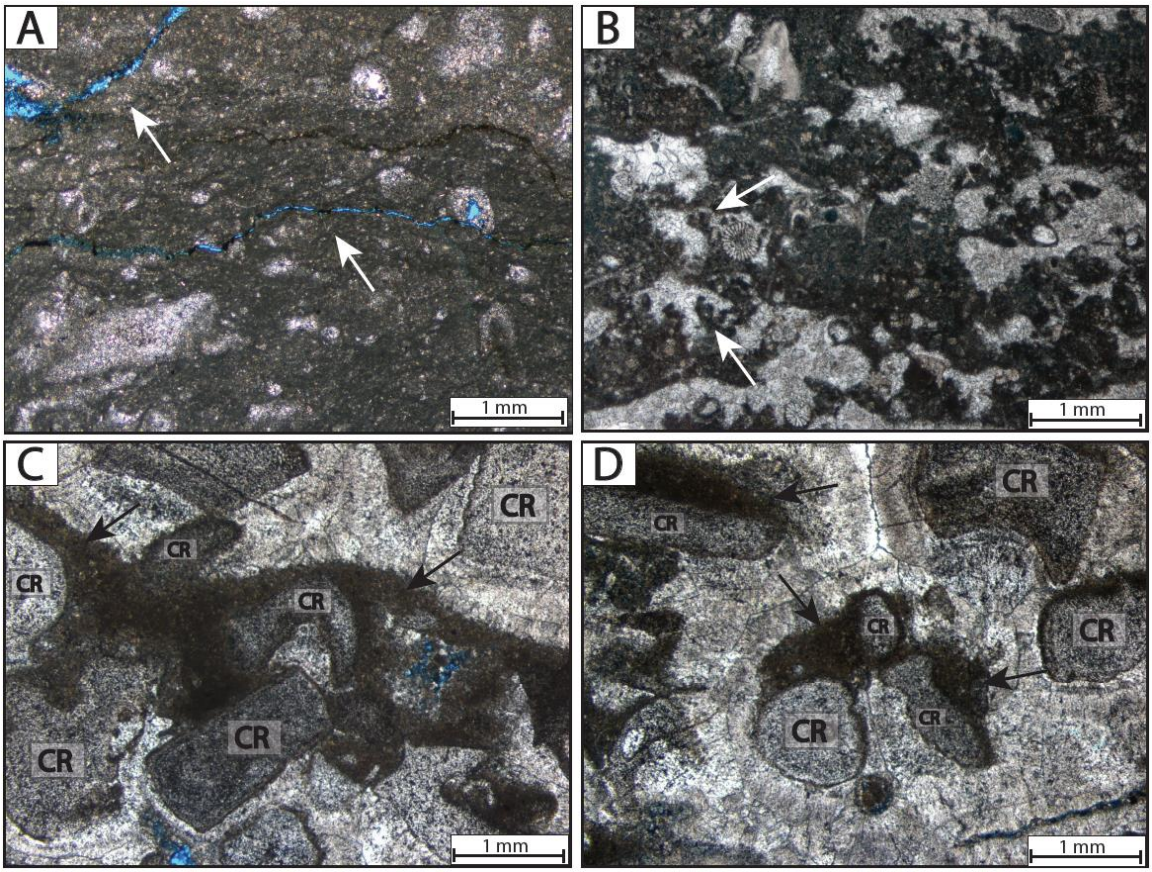

Figure 5: Photomicrographs of the Facies 1 from the forereef slopes showing: A) Layered clotted micrite with local open fractures seen through blue epoxy (white arrows). B) Various skeletal fragments in a clotted and peloidal micrite matrix with local dendritic structures (white arrows). C) Binding micrite (black arrows) locally connects crinoid grains (CR) by creating a bridge-like structure. D) In some cases, this dense micrite creates asymmetric micritic crusts on crinoid grains (black arrows) where this micrite appears to be precipitated in the upper parts of the crinoid grains based on nearby geopetal structures.

### *II. Crystalline Abiotic Cements*

There are various morphologies of crystalline cements found in the forereef slope deposits of the Pipe Creek Jr reef complex. While there is some research suggesting that all mineralogical precipitation has at the basic level the influence of microbial organisms (Buczynksi and Chafetz, 1991; Diaz et al. 2017; Flügel, 2004; Folk, 1993), the crystalline cements in this study are interpreted as abiotic and referred to as such throughout. The

various cement morphologies, stable isotopic composition (C/O), and cathodoluminescence signatures will be discussed in the following sections. For carbonate sediments and rocks, various variations of the stable isotopes of carbon and oxygen are used to differentiate the compositions of varying diagenetic fluids such as seawater, freshwater, evaporitic fluids, and burial fluids (Moore, 2001). In this study, the carbon and oxygen isotopic values reported herein are a combination of those reported by Simo and Lehmann (2000) as well as additional samples collected for the purpose of this study.

### *i. Syndepositional Abiotic Marine Cements*

Syndepositional abiotic marine cements were identified based on cement morphology and relation to other published examples (Kirkland et al. 1998, Martín et al. 1997, Flügel, 2004) which describe common syndepositional abiotic marine cements found in reef systems. These cements are most pervasive in Facies 1. Some of the predominant cement morphologies include botryoidal cements, radiaxial fibrous cements, and syntaxial overgrowths. In outcrop and hand sample, the botryoidal cements occur as large centimeter scale void-filling cements with a maximum thickness of 4 cm and minimum of 1.5 cm (Table 1). The radiaxial fibrous cements appear as grayish yellow (5 Y 8/4) to white (N9) (Goddard et al. 1970) isopachous linings (Fig. 6A) which have a maximum thickness of 2.5 cm to a minimum of 0.05 cm (Table 2). Under the petrographic microscope, the fibrous nature of these cements (Fig. 6B) exhibits a sweeping extinction in cross polarized light similar to that described by Scholle and Ulmer Scholle (2003) and Bathurst (1975). Under CL, these cements show a blocky to

weak CL, a stark contrast from the post depositional cements which have a bright CL and multiple zones (Fig. 6C).

| Botryoidal Cements | | |
|---|---|---|
| **Sample** | **Minimum Thickness (cm)** | **Maximum Thickness (cm)** |
| **Sample 5** | **1.2** | **2.5** |
| **Unmarked** | 1.2 | 4 |
| **Unmarked** | 1.2 | 2.5 |
| **Unmarked** | 1.2 | 4 |

Table 1: List of measurements of the thickness of botryoidal cements in hand sample. The thickness of these cements vary from a maximum of 4 cm to a minimum of 1.5 cm.

| Radiaxial Fibrous Cements | | |
|---|---|---|
| **Sample** | **Minimum Thickness (cm)** | **Maximum Thickness (cm)** |
| **EQ B1** | 0.1 | 0.05 |
| **EQ B2** | 0.15 | 0.3 |
| **EQ B1** | 1 | 2 |
| **WQ 16** | 0.1 | 0.2 |
| **WQ 16** | 0.1 | 0.3 |
| **WQ 16** | 0.05 | 0.2 |
| **WQ 16** | 0.3 | 0.5 |
| **WQ 16** | 0.05 | 0.1 |
| **WQ 4** | 0.2 | 0.4 |
| **WQ B** | 0.3 | 0.5 |
| **SQ A** | 0.3 | 0.5 |
| **SQ B** | 0.3 | 1 |
| **SQ B** | 0.3 | 0.25 |
| **10C** | 0.3 | 0.5 |
| **#5** | 0.5 | 2.5 |
| **#8** | 1 | 1.5 |

Table 2: List of measurements of the thickness of radiaxial fibrous cements in hand sample and thin section. The thickness of these cements vary from a maximum of 2.5 cm to a minimum of 0.05 cm.

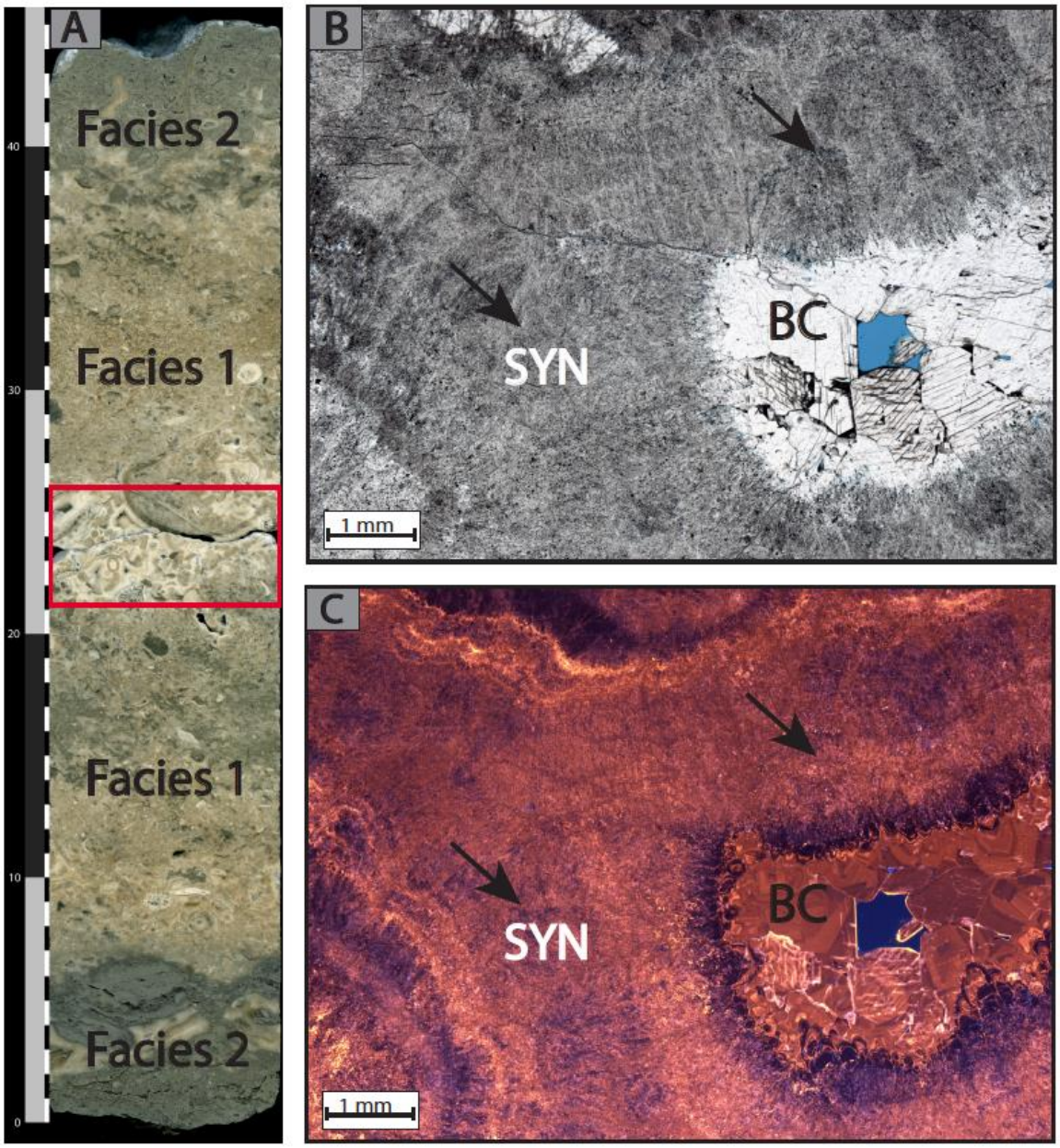


Figure 6: Syndepositional abiotic marine cements (SYN) seen in the forereef slope deposits: A) Slabbed core which depicts a transition from facies 2 to facies 1. Facies 1 is a skeletal grainstone to packstone that usually contains abundant isopachous marine cements which are outlined in the red box (Scale: 1 cm); Facies 2 is a stromatactis mudstone to wackestone; B) Isopachous linings of syndepositional radiaxial fibrous cements can reach up to a few millimeters (~3 mm) in thickness. Later stage cements include clear blocky calcite cements (BC) which are interpreted to be related to burial diagenesis. C) Same thin section image as B under CL, SYN cements show a blotchy to weak CL.

Brachiopods shells are known for storing important geochemical signatures as well as trace elements (Romanin et al. 2018). These organisms precipitate low-magnesium calcite (LMC) shells in isotopic equilibrium with ambient seawater and are resistant to diagenetic alteration (Romanin et al. 2018). Isotopic composition ($\delta^{13}C/\delta\ ^{18}O$) for brachiopod shells and micrite were obtained by Simo and Lehmann (2000) to estimate original seawater isotopic values. Samples were collected based on their homogeneous CL and minimal visible recrystallization. Brachiopod shells have isotopic values of $\delta^{13}C = 0.9 \pm 0.8‰$ and $\delta\ ^{18}O = -4.7 \pm 1.5‰$ and micrite samples have values of $\delta^{13}C = 1.2 \pm 0.3‰$ and $\delta\ ^{18}O = -5.4 \pm 0.9‰$. The radiaxial fibrous cements have mean isotopic values of $\delta\ ^{18}O = -5.4 \pm 0.9‰$ (range, - 4.2 to -7.6‰) and $\delta^{13}C = 1.3 \pm 0.5‰$ (range, 0.4 to 1.9‰) and fall within the field for estimated seawater values during the Silurian as proposed by Wenzel and Joachimski (1996) and Lohmann (1988) (Fig. 7). Other minor morphologies of syndepositional abiotic marine cements include syntaxial overgrowths. These cements occur on crinoid grains throughout the forereef slope deposits and show unit extinction with the crinoid grain from which they nucleate. These cements contain abundant randomly distributed dark inclusions which can be seen in plain polarized and cross polarized light.

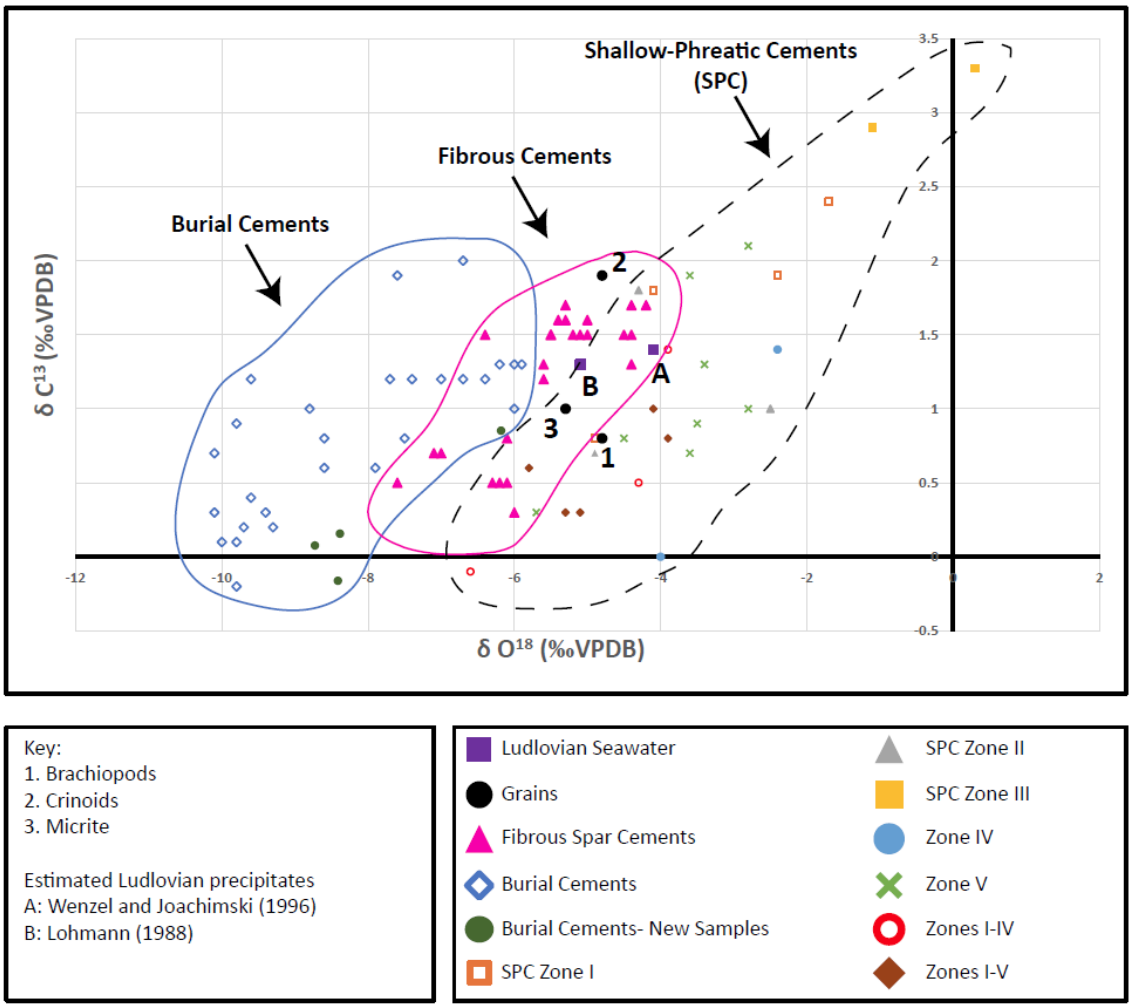


Figure 7: $\delta^{13}C$ vs. $\delta\ ^{18}O$ for skeletal grains, micrite, and cements. Location of letters A and B represent the estimates of Wenzel and Joachimski (1996) and Lohmann (1988) of carbonate precipitates from Silurian (Ludlovian) sea waters. The numbers represent mean isotopic compositions for: 1) brachiopods; 2) crinoids; and 3) micrite. Burial cements, syndepositional radiaxial fibrous cements, and shallow-meteoric phreatic cement values are also shown. Syndepositional radiaxial fibrous cements exhibit isotopic values consistent with known seawater values ($\delta^{13}C$ 1.3‰ to 1.4‰, and $\delta\ ^{18}O$ -5.1‰ to -4.1‰). Additional isotopic composition of burial cements from this study are also plotted and show isotopic values consistent with burial fluids. Modified from Simo and Lehmann (2000)

### *ii. Shallow-Meteoric Phreatic Cements*

Shallow-meteoric phreatic cements were identified based on cement morphology, CL images, as well as isotopic composition. These cements are observed in both Facies 1 and 2 and they postdate marine internal sediments and syndepositional marine cements. These occur as isopachous linings, and as previously described by Simo and Lehmann (2000), show five concentric CL zones. These zones are: (1) Zone I is non-CL with scalenohedral to rhombohedral crystal termination; (2) Zone II is characterized by bright-orange CL; (3) Zone III exhibits orange-brown to dull CL, shows crinkly lamination and scalenohedral crystal termination; (4) Zone IV is non-CL, with thin, irregular, and discontinuous bright-orange CL subzones, and (5) Zone V is characterized by dark to light-brown dull CL with rhombohedral crystal termination. Cathodoluminescence analysis of samples collected for this study (Fig. 8) clearly shows Zones I-IV as described by Simo and Lehmann (2000). Isotopic composition for these cements show a mean stable-isotope composition of $\delta\ ^{18}O$ = -3.9 ± 1.5‰ (range, -6.7 to 0.4‰) and $\delta^{13}C$ = 1.3 ± 0.9‰ (range, -0.2 to 3.1‰). These isotopic values coincide with values for meteoric waters which range in $\delta\ ^{18}O$ from -4 to -2‰ and in $\delta^{13}C$ from −20 to +20‰ (Moore, 2001). These shallow-meteoric phreatic cements are enriched in $\delta^{13}C$ and $\delta\ ^{18}O$ relative to their marine precursors.

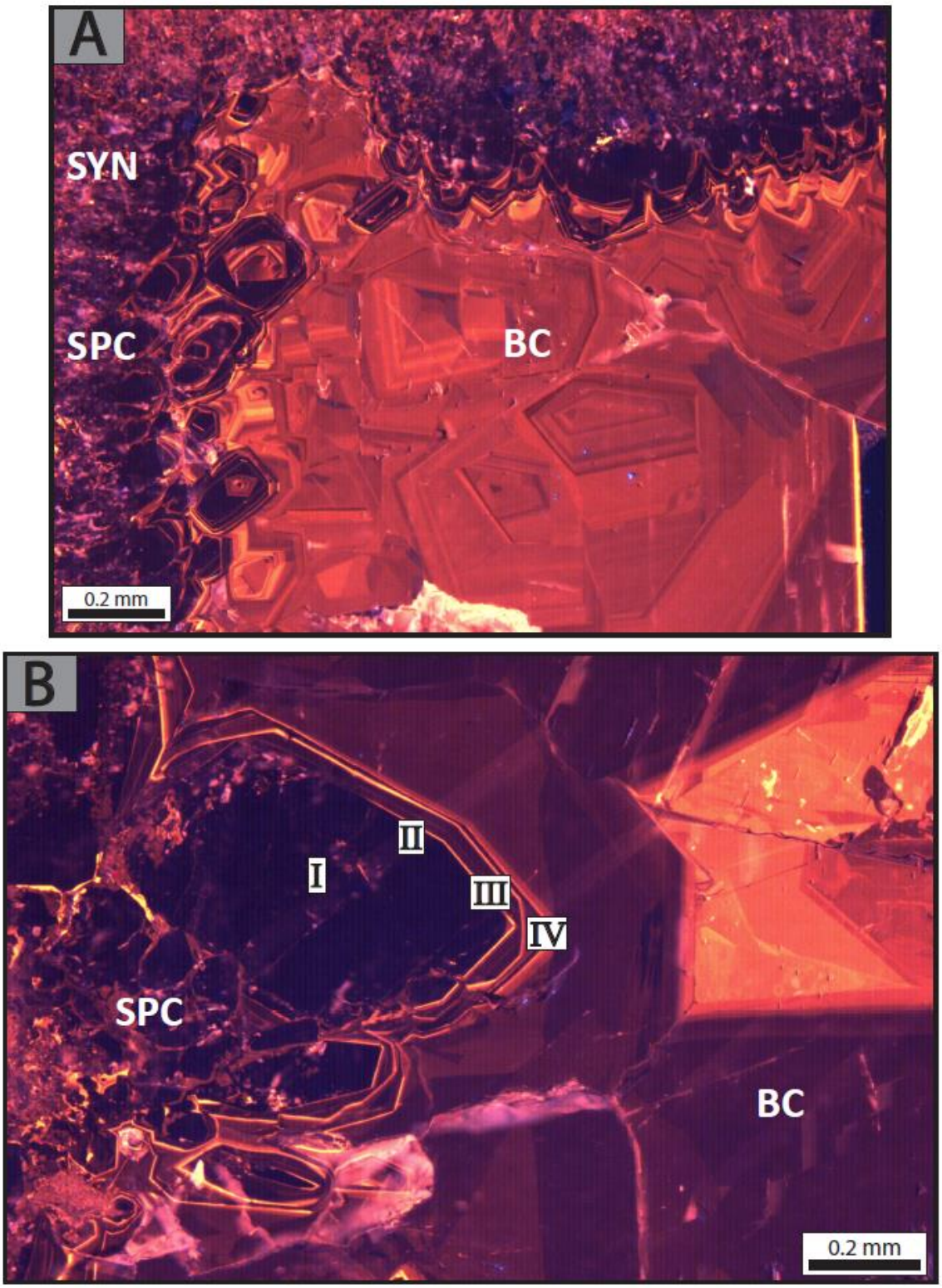


Figure 8: CL photomicrographs. A) Syndepositional radiaxial fibrous cements (SYN) show blotchy to weak CL while shallow-meteoric phreatic (SPC) and burial cements (BC) show variations of bright and dull CL. B) SPC Zones I-IV are consistent with what

was identified by Simo and Lehmann (2000). BC zones show concentric and sectoral zoning as well as multiple zonations.

### *iii. Burial Cements*

Burial cements are observed in both Facies 1 and 2 of the forereef slope deposits. These cements superimpose all cement types and are visible as clear limpid calcite cements under the petrographic microscope. Using CL, Simo and Lehmann (2000) were able to identify up to seven alternations of orange to brown dull CL colors and discontinuous corrosion surfaces at the base of the dark-brown zones. These zones show concentric and sectoral zoning (Reeder and Paquette, 1989). A direct comparison of the CL zones described by Simo and Lehmann (2000) with new samples collected for this study was not successful, nevertheless the multiple zonations characteristic of these cements could be observed (Fig. 8). These cements have a mean isotopic composition of $\delta\ ^{18}O$ = -8.2 ± 1.5‰ (range, -10.2 to -6.0) and a mean $\delta^{13}C$= 0.9 ± 0.6‰ (range, -0.5 to 2.1) as reported by Simo and Lehmann (2000). Samples of these cements analyzed In this study have a mean isotopic composition of $\delta\ ^{18}O$ = -7.9 ± 1.1‰ and $\delta^{13}C$= 0.44 ± 0.2‰. These isotopic values coincide with isotopic values reported for burial cements which have $\delta^{18}O$ values from -4 to -10‰ and $\delta^{13}C$ values from 1 to 5‰ (Moore, 2001).

*Syndepositional Cements and Microbial Binding in Various Locations of the Pipe Creek Jr. Reef Complex*

Samples of the forereef slope deposits were analyzed from the 3 accessible quarry pits (West, East, and South) to compare facies and the types and relative abundance of syndepositional cementation and microbial binding. Facies 1 and 2 were present in all 3 locations of the quarry.

*i. West Pit*

Samples from the West Pit consist of up to 60% cement (abiotic and microbial) (Table 3). The microbial micrite is dense and locally laminated, and displays distinct repetitive fabrics which include bridge-like structures of lithified dense micrite that locally connect bioclasts (Fig. 9). Evidence of early lithification is seen by the preservation of primary porosity that was later occluded by syndepositional and postdepositional abiotic cements (Fig. 9A). Other fabrics include dense micrite which appears to trap and connect different crinoid grains (Fig. 9B) as well as micritic crusts which show better development in the upper part of the bioclasts based on geopetal structures (Fig. 9C-D).

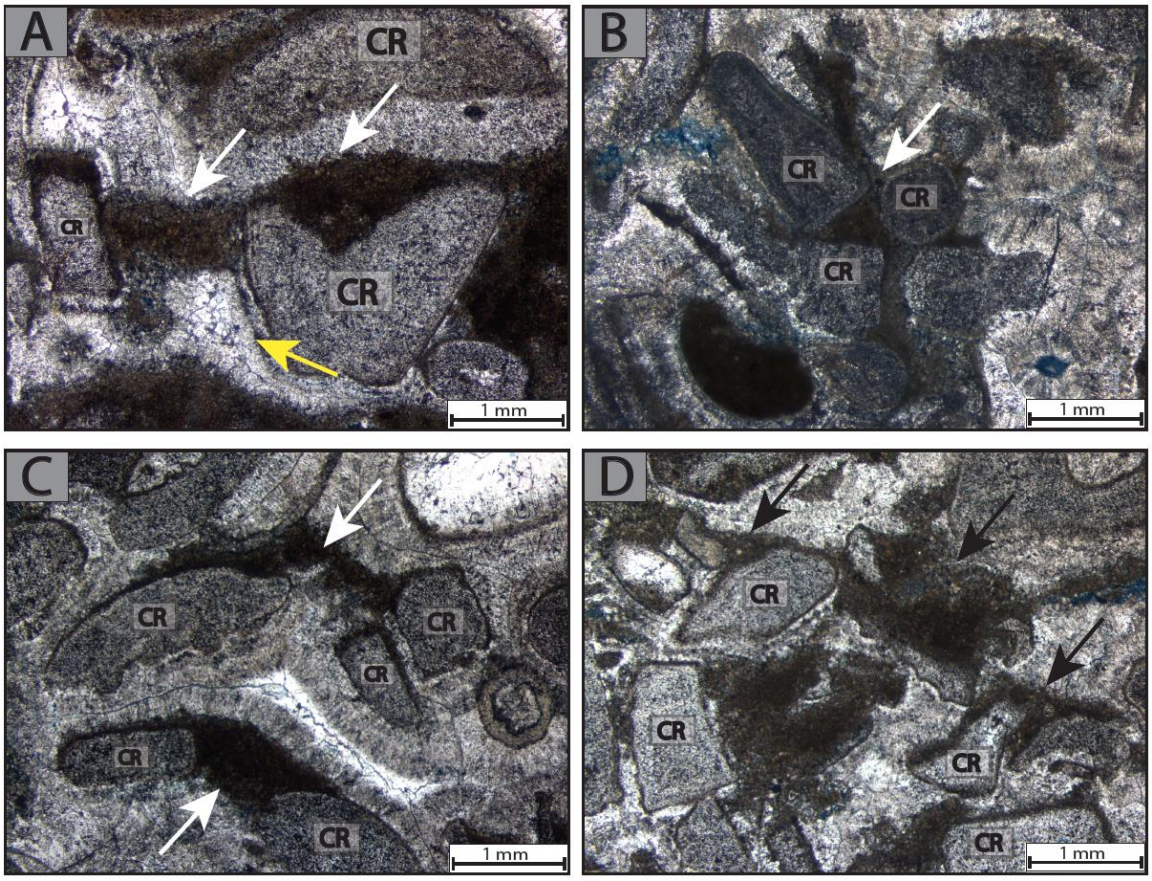

Figure 9: Photomicrographs of the dense micrite in samples collected from the West Pit of the Pipe Creek Jr. Quarry: A) Micritic bridge-like structures (white arrows) are observed locally connecting bioclasts, in this case crinoid grains (CR). This micrite appears to be lithified early and allows for the preservation of an internal cavity (yellow arrows) which is later occluded with abiotic marine cements. B) Dense micrite is observed acting as a trapping mechanism with crinoid grains (white arrows). C) This dense micrite frequently appears as bridge like structures binding (white arrows) crinoid grains and may show some degree of preferential precipitation. D) Micritic crusts on crinoid grains show better development on the upper parts (top) of the crinoid grains (black arrows) based on geopetal structures.

Syndepositional abiotic (crystalline) marine cement consists of isopachous linings with a radiaxial fibrous nature (Fig. 10). Sweeping to unit extinction under cross polarized light (Fig. 10B and D) indicates that this cement was partially to fully recrystallized (Bathurst, 1975). This is also noted under CL by the presence of microdolomite inclusions in these cements. The relative abundance of the varying cement morphologies and micrite found in the West Pit can be found in Table 3.

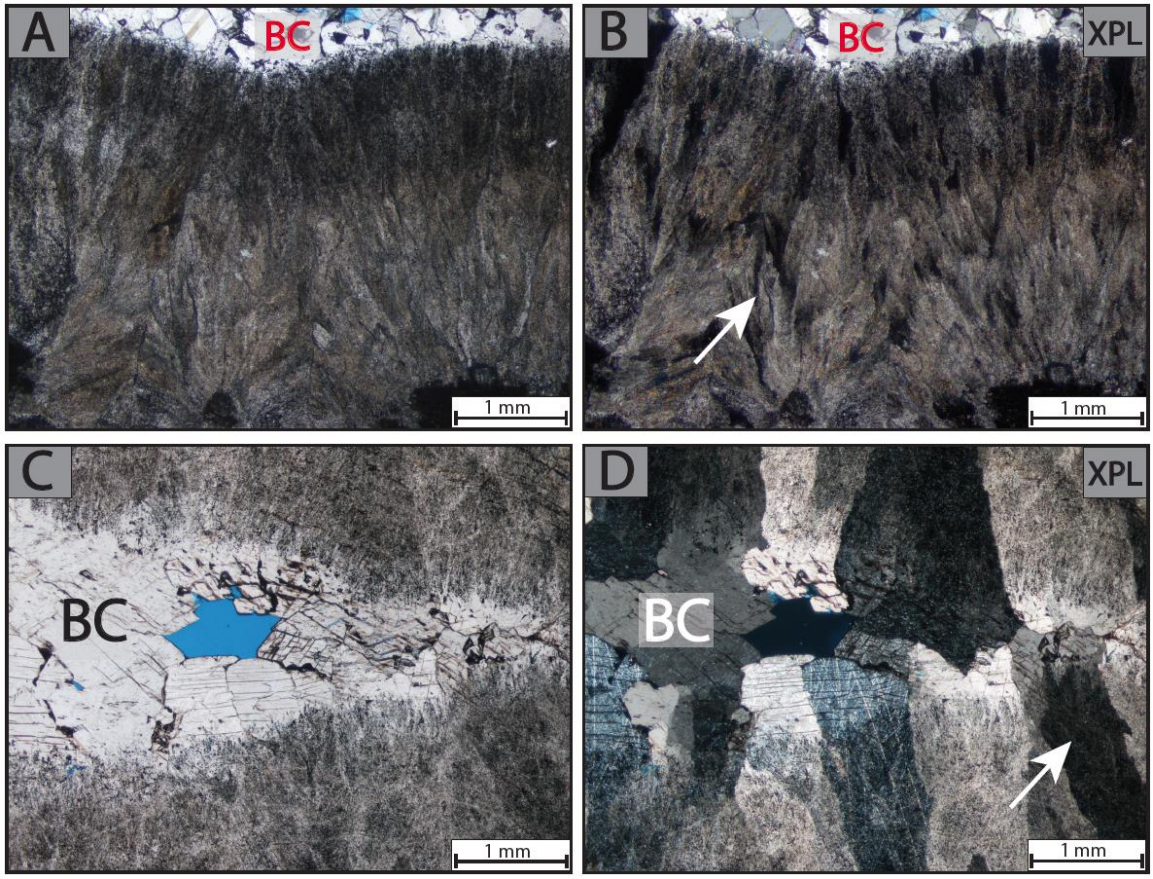

Figure 10: Photomicrographs of syndepositional abiotic marine cements in samples collected from the West Pit of the Pipe Creek Jr. Quarry: A-B) Fully neomorphosed radiaxial fibrous cements show a sweeping extinction under cross polarized light and can be a few millimeters in thickness (white arrow). C-D) Recrystallized radiaxial fibrous cements are distinguished by their unit extinction under cross polarized light (white arrows). Radiaxial fibrous cements are followed by late stage blocky calcite spars (BC).

| Relative Abundance of Cement Morphologies and Micrite: West Pit | | | | | |
|---|---|---|---|---|---|
| **Sample** | **Radiaxial Fibrous (%)** | **Syntaxial Overgrowths** | **Botryoidal** | **Blocky Spar** | **Microbial Micrite** |
| **WQ Block 19** | 50 | 0 | 0 | 0 | 50 |
| **WQ Block 16** | 90 | 0 | 0 | 0 | 10 |
| **WQ_PC1E** | 100 | 0 | 0 | 0 | 0 |
| **WQ_PCO1A** | 95 | 0 | 0 | 0 | 5 |

Table 3: Relative abundance of cement morphologies in thin sections from the West Pit. The most abundant cement morphology is radiaxial fibrous. Samples from the West Pit also have a significant amount of microbial micrite (highest of 50%).

Scanning electron microscopy of ion-milled samples from the forereef slopes exposed at the West Pit reveals microbial features such as fossilized bacterial communities, bacterial filaments, and microbial biofilms found along the edges and walls of remaining pore space. These were identified based on morphological traits as personally communicated by Dr. Mara Diaz of the Department of Marine Geosciences, Rosenstiel School of Marine and Atmospheric Science at the University of Miami, and by comparison with relevant literature (Diaz et al. 2017, Gebhardt et al. 1954, Harris et al. 2019, and Westall et al. 2001). Some of the fossilized bacterial communities include filamentous cyanobacteria which are identified by a slightly curved shape (Fig. 11A) that form binding structures. These filamentous cyanobacteria range in length from 1-2 µm with larger filaments exceeding 2 µm. Rod-shaped <1 µm long features are interpreted as fossilized bacterium (Fig. 11B), with some interpreted as entombed bacterium identified as *Coccoid* shaped bacteria (Fig. 11C). *Coccus* is one of the major basic shapes of bacteria and is characterized by a seed-like spherical or oval shape (Gebhardt et al. 1954). This shape of bacteria forms distinct groupings based on their planes of division (Gebhardt et al. 1954). Some of these include diplococcus or double seed and streptococcus which forms curved or flexuous seed grouping (Gebhardt et al. 1954). Further structures include micritic bridge-like structures that extend from the surfaces of remaining pores and measure 1-2 µ in length (Fig. 11C). Features interpreted as fossilized biofilms such as extracellular polymeric substances (EPS) were also observed (Fig. 11B). Extracellular polymeric substances or biofilms are produced by microbes and accumulate on the outside of cells to form a protective and adhesive matrix that attaches

microorganisms to substrates, provide physical and chemical protection, and aid in the absorption of nutrients (Riding, 2000).

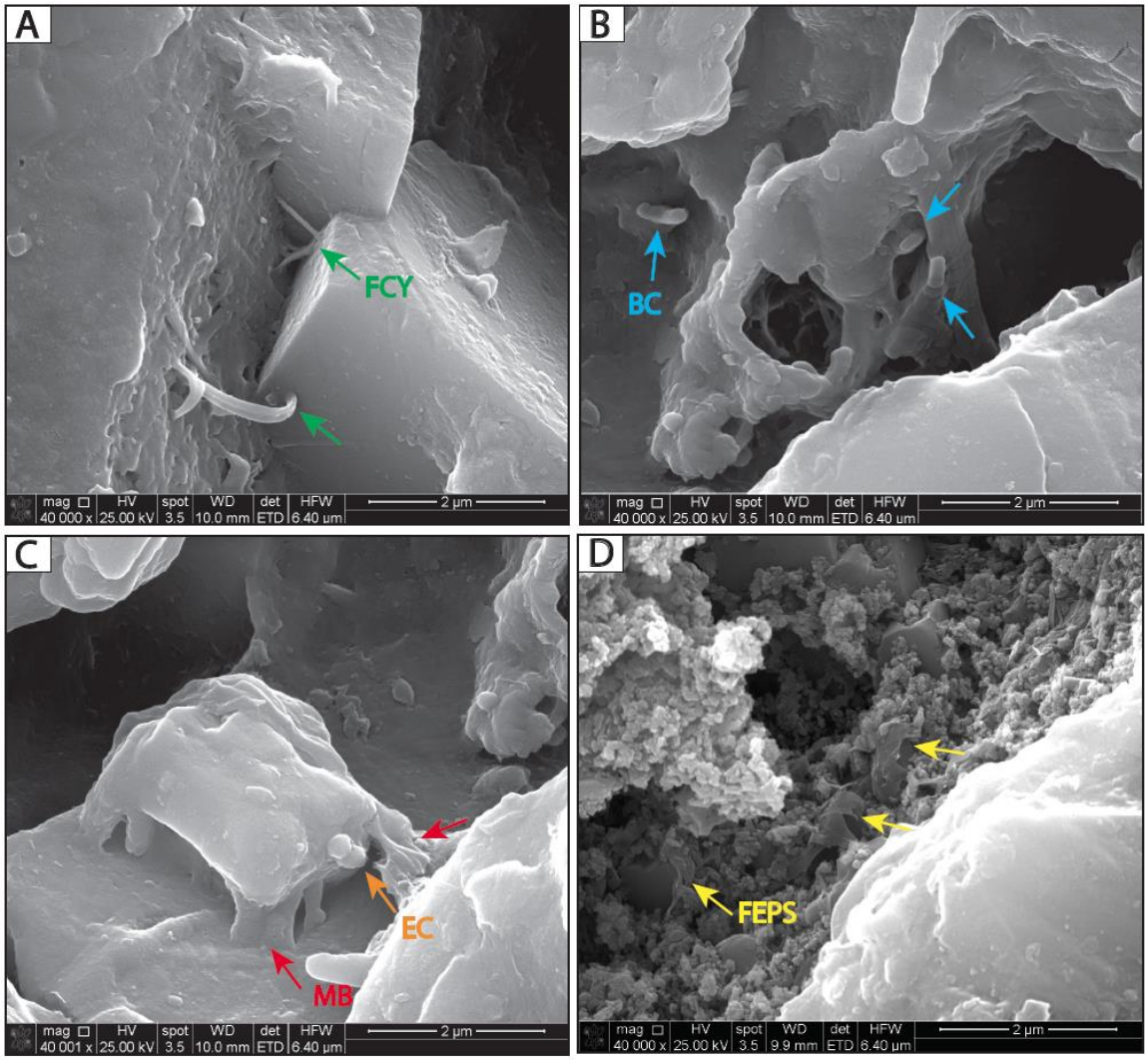


Figure 11: SEM images of ion-milled samples of the forereef slope deposits of the West Pit: A) Green arrows depict filamentous cyanobacteria fossils (FCY), some of which are slightly curved. Some of these filaments bind calcite crystals to the pore surface. B) Blue arrows show fossilized bacterium (BC). C) Micritic bridges (MB) creating binding structures extending from the bottom and walls of the pore (red arrows). Entombed coccus shaped bacteria (EC) (orange arrows) can also be seen. D) Fossilized extracellular polymeric substances (FEPS) within remaining porosity (yellow arrows). Scale bar in all photomicrographs is 2 microns.

*ii. East Pit*

Samples from the East Pit consist of up to 40-50% cement (abiotic and microbial) (Table 4). The microbial micrite is dense to clotted and in most cases creates patches that connect and trap crinoid grains (Fig. 12A). Fabrics seen in this micrite include binding

micrite which creates bridge-like structures that can extend and connect various bioclasts and have a semi-layered appearance (Fig. 12B-D). This micrite appears to have lithified early and preserves initial cavities that have been occluded by further abiotic cements (Fig. 12B-C).

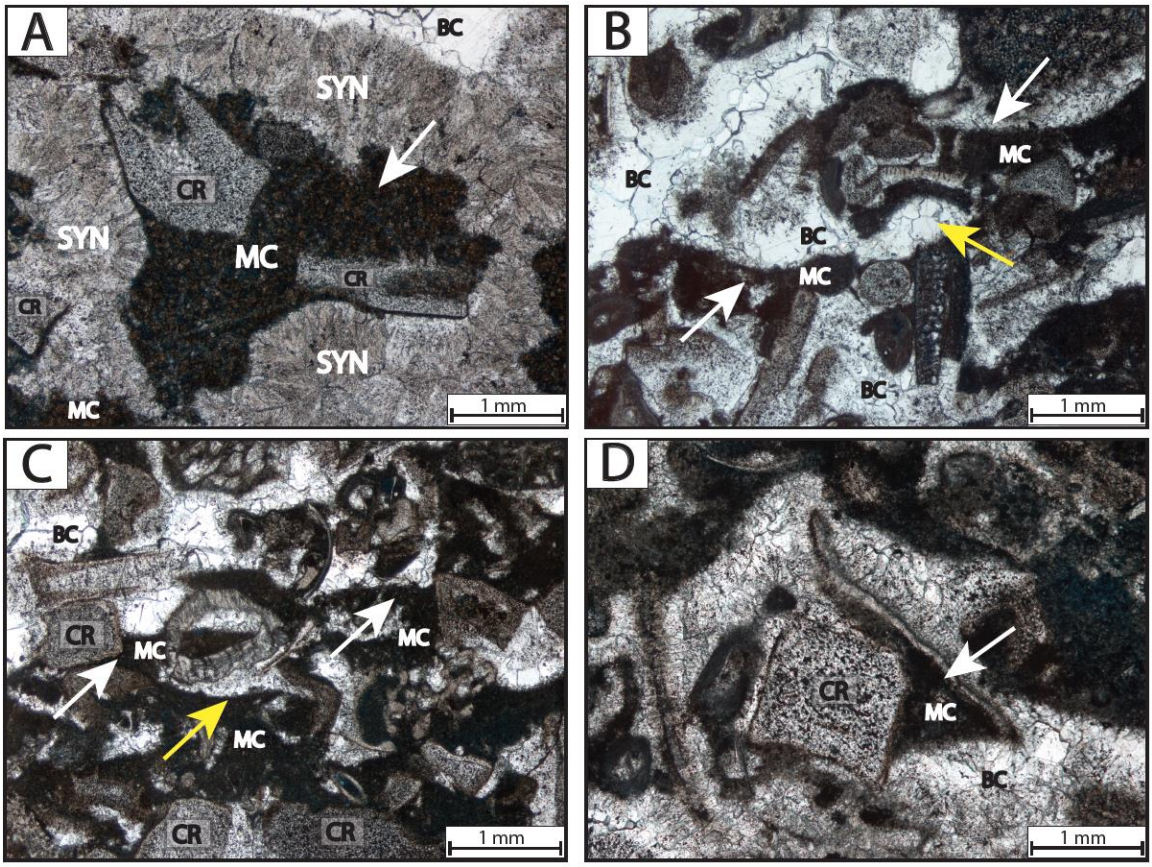


Figure 12: Photomicrographs of the dense micrite in samples collected from the East Pit of the Pipe Creek Jr. Quarry: A) Sample of Facies 1 where the dense micrite matrix (MC/white arrow) connects crinoid grains (CR). Syndepositional radiaxial fibrous cements (SYN) surrounds the dense micrite matrix. B-D) Micrite bridges composed of dense micrite (white arrows) are common and can preserve some of the original porosity which was occluded by abiotic marine cements (yellow arrow) such as clear blocky calcite (BC).

The syndepositional abiotic (crystalline) marine cements seen in the samples from the East Pit are mostly radiaxial fibrous in nature. These occur as isopachous linings in bioclasts and occluded primary porosity. Radiaxial fibrous cements are characterized by their sweeping extinction in cross polarized light and are partially recrystallized (Fig. 13).

Minor components to the syndepositional abiotic marine cements include syntaxial overgrowth on crinoid grains which can be identified by its unit extinction under cross polarized light. The relative abundance of the varying cement morphologies and microbial micrite found in the East Pit can be found in Table 4.

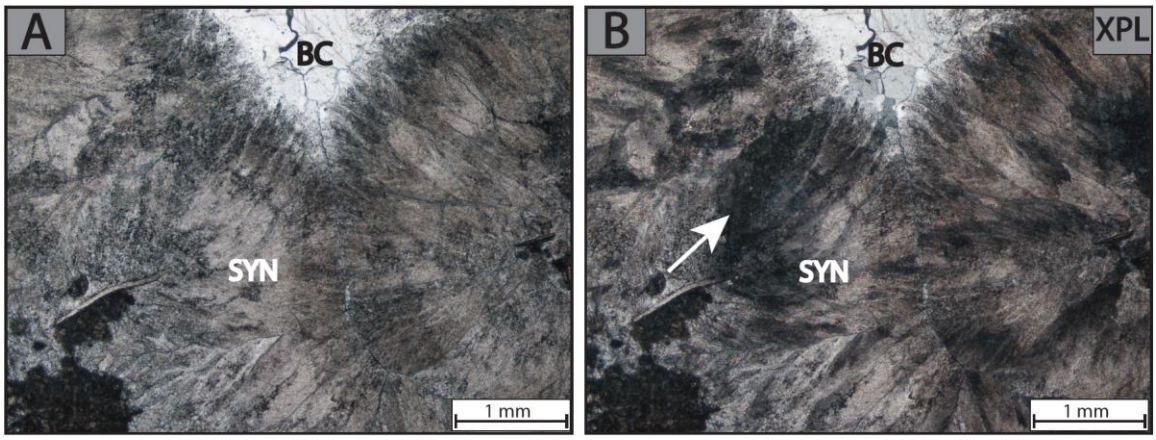


Figure 13: Photomicrographs of the syndepositional abiotic marine cement found in samples from the East Pit of the Pie Creek Jr. quarry: A-B) Partially recrystallized syndepositional radiaxial fibrous cements (SYN) show a sweeping extinction under cross polarized light (white arrows). Later stage cements include clear blocky calcite cements (BC).

| Relative Abundance of Cement Morphologies and Micrite: East Pit | | | | | |
|---|---|---|---|---|---|
| **Sample** | **Radiaxial Fibrous (%)** | **Syntaxial Overgrowths** | **Botryoidal** | **Blocky Spar** | **Microbial Micrite** |
| **EQ_C** | 5 | 5 | 0 | 90 | 0 |
| **EQ_B1** | 90 | 0 | 0 | 0 | 10 |
| **EQ_B2** | 90 | 0 | 0 | 10 | 0 |

Table 4: Relative abundance of cement morphologies in thin sections from the East Pit. The most abundant cement morphologies are radiaxial fibrous and blocky spar cements.

Scanning electron microscopy of ion-milled samples reveals microbial features such as fossilized microbial biofilms and various bacterial communities in the forereef slope deposits in the East Pit as well. Smooth sheet-like layers (Fig. 14A) and mucus-like coatings (Fig. 14B) are interpreted as biofilms or fossilized extracellular polymeric

substances (EPS). Curved structures that range in length from 0.5-1 µm are interpreted as filamentous cyanobacteria (FCY) (Fig. 14B). Other structures include rod-shaped <1 µm long features which are interpreted as fossilized bacterium (BC) (Fig. 14B).

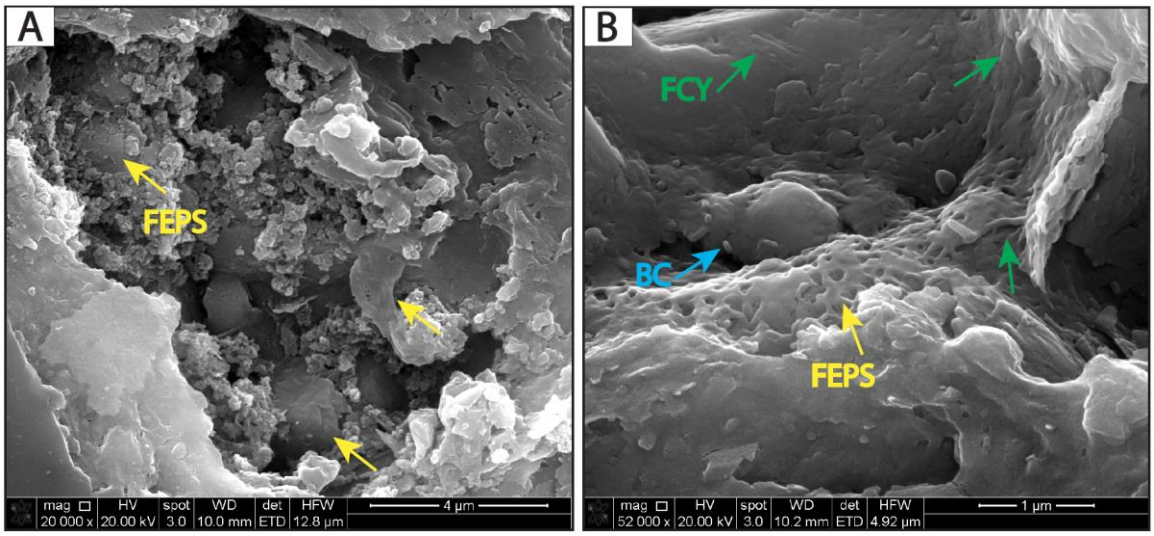


Figure 14: SEM images of ion-milled samples of the forereef slope deposits from the East Pit: A) Fossilized extracellular polymeric substances (FEPS) in association within remaining porosity (yellow arrow). B) Fossilized mucus-like EPS (FEPS) lining remaining porosity (yellow arrows). In some cases, this FEPS contains fossilized bacterial communities which include filamentous cyanobacteria denoted as FCY (green arrows) and bacterium denoted by BC (blue arrow). Scale bar is 4 microns; Scale bar is 1 micron.

*iii. South Pit*

Samples from the South Pit consist of up to 70-80% of crystalline abiotic cements. Bioclasts, mostly crinoid grains, have syntaxial overgrowth cements which are identified by their unit extinction (Fig. 15) in cross polarized light (Flügel, 2004). These cements occur in optical continuity with their host grain (e.g. crinoids) and are inclusion-rich (Flügel, 2004). Other minor syndepositional cement morphologies include thin (<1 mm) layers of radiaxial fibrous cements. The relative abundance of the varying cement morphologies and micrite found in the East Pit can be found in Table 4. In these samples many of the bioclasts, mostly crinoid grains, appear to be partially to fully micritized.

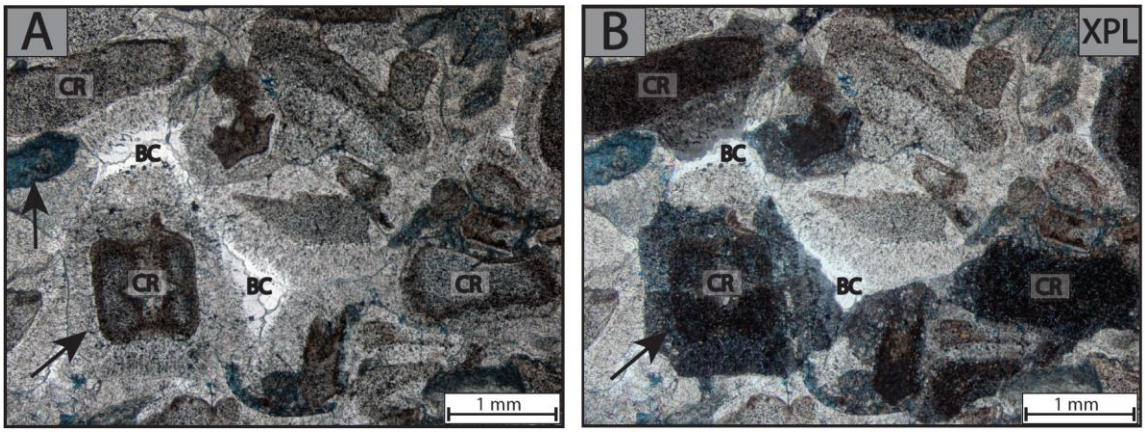

Figure 15: Photomicrographs of the syndepositional abiotic marine cement found in samples from the South Pit of the Pipe Creek Jr. Quarry: A-B) Sample of the coarse grainstone-packstone facies that shows syntaxial overgrowth cements (black arrows) on crinoid grains (CR). This cement morphology can be easily identified by its unit extinction in cross polarized light (black arrow). Later stage cements include blocky clear calcite cements (BC). Some of the remaining porosity is displayed by blue epoxy.

| Relative Abundance of Cement Morphologies and Micrite: South Pit | | | | | |
|---|---|---|---|---|---|
| **Sample** | **Radiaxial Fibrous (%)** | **Syntaxial Overgrowths** | **Botryoidal** | **Blocky Spar** | **Microbial Micrite** |
| **SQ Unmarked_01** | 0 | 20 | 0 | 80 | 0 |
| **SQ Unmarked_02** | 0 | 85 | 0 | 15 | 0 |
| **SQ_A** | 0 | 100 | 0 | 0 | 0 |
| **SQ_B** | 10 | 80 | 0 | 10 | 0 |

Table 5: Relative abundance of cement morphologies in thin sections from the South Pit. The most abundant cement morphologies are syntaxial overgrowth cements and blocky spar cements.

Scanning electron microscopy of ion-milled samples of the South Pit reveals microbial structures such as micritic bridge-like structures and fossilized bacterial communities in the forereef slope deposits. Micritic bridge-like structures are seen in remaining open pore space and range from 2 to 4 µm in length (Fig. 16A). Some of the fossilized bacterial communities include sub-spherical shaped features which are interpreted as fossilized *coccus* (FC) shaped bacteria (Fig. 16C). The size of these

interpreted fossilized *coccoid* shaped bacteria range from 0.5 to 2 µm in length. Polygonal honeycomb-like sheets interpreted as fossilized EPS (FEPS) were also identified (Fig. 16B). Other features include slightly curved-shape structures that range in length from 0.5 to 2 µm (Fig. 16C-D) which are interpreted as fossilized filamentous cyanobacteria (FCY). These FCY protrude from the surfaces of the pores and create entanglements of colony-like structures (Fig. 16D).

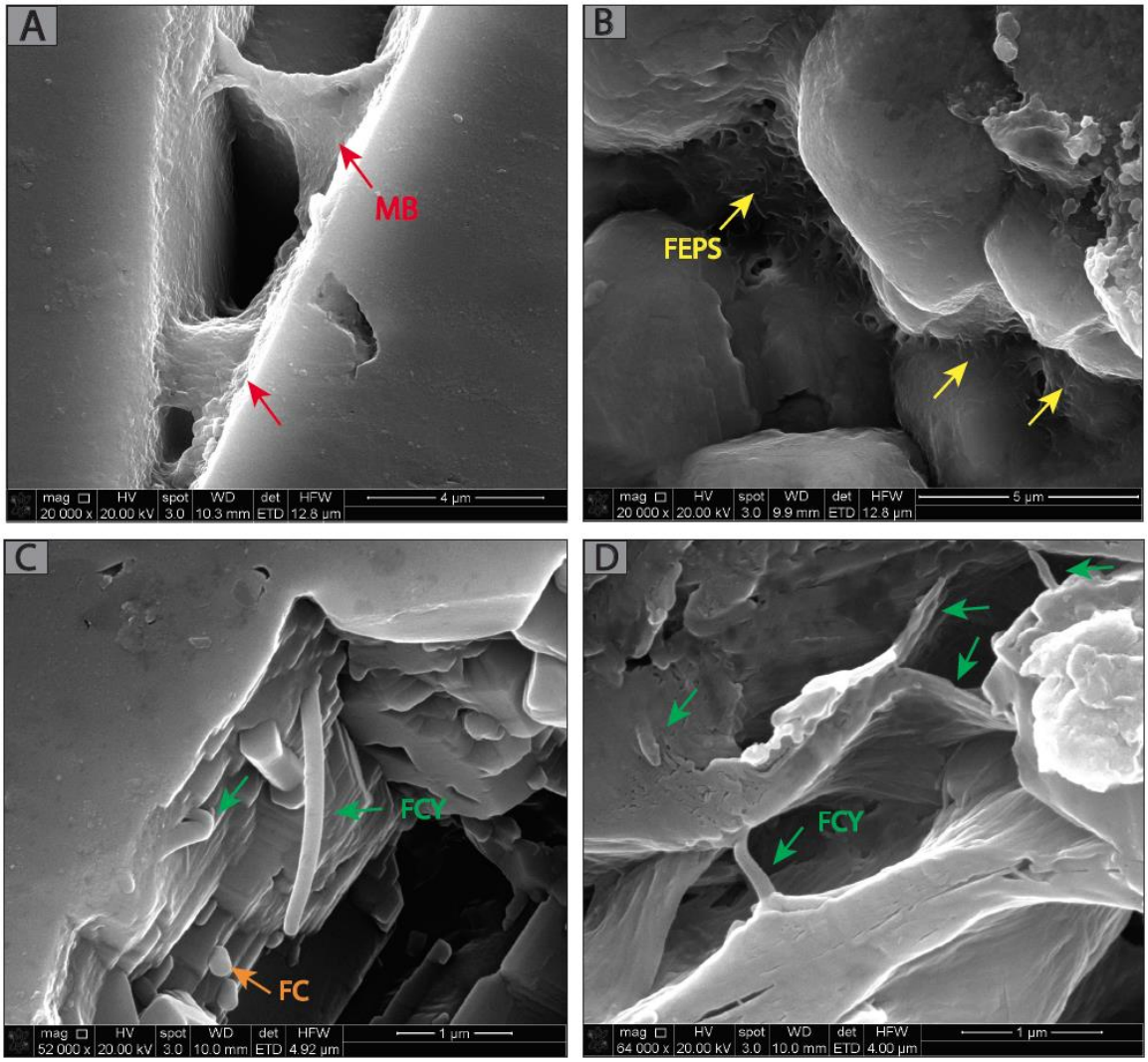


Figure 16: SEM images of ion-milled samples of the forereef slope deposits from the South Pit: A) Micritic bridges (MB) create a binding structure that extends from the surfaces of pores (red arrows). B) Fossilized EPS (FEPS) has a honeycomb-like polygonal appearance (yellow arrows). C) Fossilized bodies of cyanobacteria (FCY) have a slightly curved appearance and attach and protrude from the pore surfaces (green

arrows). In some cases the FCY appear in conjunction with fossilized *coccus* (FC) shaped bacteria. D) Green arrows depict an entanglement of mineralized filamentous cyanobacteria (FCY) which form colony-like structures. A: Scale bar is 4 microns; B: Scale bar is 5 microns; C-D: Scale bar is 1 micron

# CHAPTER IV

# DISCUSSION

## *Microbial Binding in Forereef Slopes*

Extensive microbial influence in the binding and stabilization of the steep (35-45°) forereef slope deposits of the Pipe Creek Jr. complex is seen through petrographic analysis by the presence of distinct microfabrics which have been documented in other studies (Reolid et al. 2017; Riding 2000). These microfabrics include 1) trapping and binding structures (Figs. 5C-D, 9, and 12), 2) clotted-dense micrite patches that locally connect bioclasts and preserve primary porosity (Figs. 5C-D, 9A, C-D, and 12B-D), 3) micritic crusts (Figs. 5D and 9C-D), and, 4) peloidal micrite with localized dendritic textures (Fig. 5B). All of these microfabrics fall into the category of cryptic microbial carbonates that lack distinctive macrofabrics, but typically possess micritic, clotted, or peloidal microfabrics that may also contain traces of filaments (Riding 1991). Microbial influence in the binding and stabilization of these forereef slopes inhibits slope failure and preserves the steep angles of these deposits.

Trapping and binding structures have been described by Reolid et al. (2017) as being related to microbial influence. These structures are related to microbial processes, more specifically the adhesion of sediment due to the sticky nature of extracellular polymeric substances (EPS) produced by microbes (Riding 2000). The terms 'trapping and binding' are commonly used in the stromatolite literature to indicate initial preservation of sediment on a microbial substrate (Riding 2000). The presence of fossilized EPS in samples of the forereef slopes collected from the three pits of the Pipe Creek Jr. quarry further suggest a microbial origin (Figs. 11D, 14, and 16B). Multiple EPS samples were analyzed under the ESEM and showed compositions of 44.05%, 46.82%, 48.35%, and 98.97% calcium, with little to no silicon, potassium or aluminum, confirming that these coatings are not authigenic clays. The full elemental analyses of these EPS samples can be found in the appendix.

Micritic crusts or micrite envelopes have also been described as a result of microbial processes (Riding, 2000), specifically the calcification of biofilms (EPS). These microfabric are observed in samples from the Pipe Creek Jr. reef complex (Fig. 5C-D and 9C-D) and could be related to distinct phototrophic microorganisms that require light energy to photosynthetically fix carbon (Riding, 2011). Similar fabrics are seen in the Holocene of the TOTO (Bahamas) where samples show micritic crusts of varying thicknesses developed preferentially on different sides of the *Halimeda* plates. Other examples include modern forereef slopes in the Red Sea where micrite crusts form isopachous layers on upper surfaces of ledges (Brachert and Dullo, 1991). The crusts found in the Red Sea are reported to have formed *in situ* by biogenic processes which are indicated through SEM analysis by the presence of calcified bacterial/fungal filaments

and probable *coccoid* shaped algae and bacteria which bind the sediment (Brachert and Dullo, 1991).

The dense and clotted micrite fabrics observed in all three pits (Fig. 11, 14, and 16) are also likely of microbial origins, and includes calcified EPS and microbial sheaths (e.g. cyanobacteria), along with calcified bacterial cells (Riding, 2000). These types of fabrics have also been described as a main component in the Late Miocene *Halimeda*-microbial boundstones in the Sorbas Basin of Spain (Martín et al. 1997). Peloidal micrite with dendritic textures is related to calcified bacterial aggregates (Macintyre, 1985 and Riding 2000) with dendritic fabrics resulting from cyanobacterial calcification (Riding 1991). The presence of fossilized cyanobacteria in samples of the forereef slope deposits at Pipe Creek Jr. suggest a microbial origin of the dendritic microfabric (Fig. 11A, 14B and 16C-D). Similar peloidal fabrics have described in subsurface examples, including the *in situ* microbial boundstone facies of the steep (~45°) Upper- to Middle- slope of the Late Visean to Bashkirian Tengiz Field in the Precaspian Basin, Kazakhstan (Collins et al. 2006). Other examples include the Middle and Upper Capitan Formations of the Permian El Capitán reef in West Texas where gravity defying peloidal micrites are interpreted to be precipitated within mucilaginous microbial aggregations (Kirkland et al. 1998).

Petrographic analysis of these microfabrics suggest that they are precipitated early during deposition, whereas scanning electron microscopy of surficial microbial fabrics are less clear from a paragenetic standpoint. Later stage diagenetic fluids could be responsible for the surficial microbial features observed in SEM. The Pipe Creek Jr. reef complex clearly has had a complex diagenetic history which involves multiple stages of

cementation such as syndepositional abiotic marine cements, shallow-meteoric phreatic cements, postdepositional burial cements, karsting and dissolution, and hydrocarbon emplacement and migration (Simo and Lehmann 2000). A recent study documents that crude oil lenses can contain bacteria supplied to reservoirs by infiltration of surface waters and can also contain bacteria that is autochthonous to the environment of crude oil and formation waters (Wolicka and Borkowski 2012). Further biogeochemical work (e.g. shot-gun metagenomic DNA analyses and sequencing analyses) can aid in the timing and identification of the bacterial communities present in these samples (Diaz, 219, pers. communication).

*Early Lithification of Microbial Binding*

Petrographic analysis of the forereef slope deposits exposed at the Pipe Creek Jr. reef complex show evidence of early lithification. Based upon the distribution of micritic bridge-like structures relative to the "later" abiotic cements, the microbial stabilization and lithification happened early and allowed for the preservation of internal cavities and initial porosity that was later mostly occluded with abiotic marine cements (Fig. 7A, C-D, and Fig. 12B-D). This early lithification due to microbial binding has been reported in steep carbonate slopes of the Holocene TOTO (Bahamas) and the upper Miocene of the Cariatiz Platform (Spain) where microbial micrite was lithified during deposition, thus preserving open pore spaces (Fig. 17). Other examples include the Middle and Upper Capitan Formations of the Permian Capitan reef where gravity-defying micrite is lithified at very steep angles (55° to 80°) and is responsible for the preservation of open pore space that was later filled by botryoidal aragonite cements (Kirkland et al. 1998).

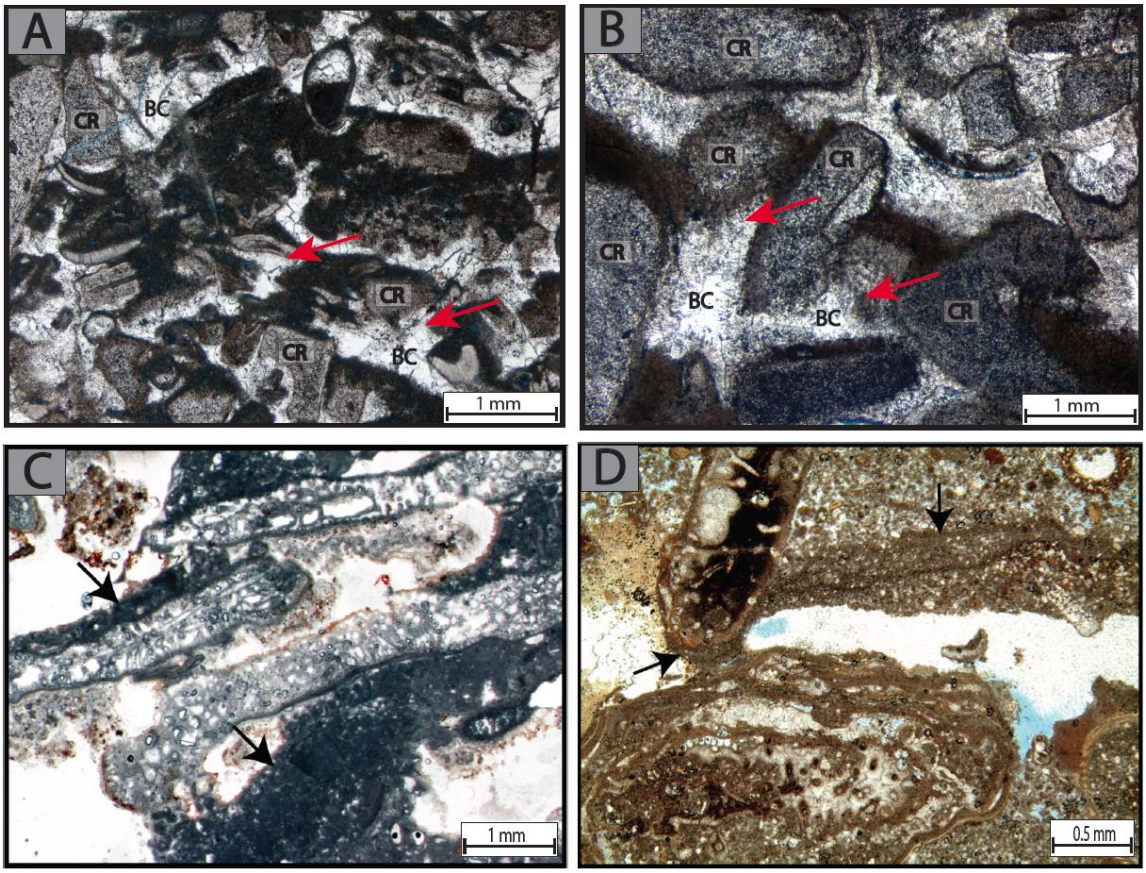


Figure 17: Comparison of early lithified microbial micrite from the Silurian forereef slopes of the Pipe Creek Jr. reef complex (A-B) and samples from the Cariatiz (C) and TOTO slopes (D) from Reolid et al. 2017. A-B) Early lithification of dense micrite bridges allows for the preservation of previously open pore space occluded by clear blocky calcite cements (BC) (red arrows). C) Samples from the Cariatiz slopes show clotted to dense micrite (black arrows) that connect *Halimeda* plates and preserve the primary interparticle porosity in these deposits. D) *Halimeda* floatstone from TOTO slopes show microbial binding that preserves an internal cavity (black arrow). Large grain in lower left shows microbial binding and encrustation of a *Halimeda* plate.

*Paragenetic Relationship of Microbial Binding and Syndepositional Abiotic Marine Cements*

Reolid et al. (2017) propose that the presence of microbial binding in steep slopes of the Holocene TOTO (Bahamas) and the Miocene of the Cariatiz Platform (SE Spain) is a factor in the early stabilization of carbonate slopes deposited at steep angles of repose. This binding essentially occurs before the stabilization by abiotic marine cements during the first hundreds of years after deposition (Reolid et al. 2017, Grammer et al. 1993 a and b). Petrographic analysis of the Pipe Creek Jr. slope deposits reveals a visual paragenetic relationship which confirms that microbial binding precedes further stabilization by syndepositional abiotic marine cements as discussed above (Fig. 4). While this relationship is clearly determined through petrographic analysis, SEM analysis of ion milled and non-milled samples of microbial structures lining pores and pore throats is not unequivocally early. Nevertheless, the presence of filamentous cyanobacteria that appears to be binding calcite crystals to pore surfaces, micrite bridges and EPS coatings of pore space suggest that microbial binding and syndepositional abiotic marine cements are important processes in the formation and stabilization of steep carbonate slopes (Figs. 11A & C, 14, and 16A-B).

*Windward vs. Leeward Variability*

Comparison of the relative abundance and morphologies of syndepositional abiotic marine cements in the three pits of the Pipe Creek Jr. quarry (West, East, and South) reveals variations possibly due to windward and leeward orientations of the reef complex. The recognition of windward and leeward variability in ancient and modern

reefs has been well documented (Gischler, 1995; James et al. 1976; Grammer et al. 1993a; Trout et al. 2017; Wold and Grammer, 2017). Early studies by Darwin (1842) recognize the significance of prevailing winds and currents in the arrangement of leeward and windward margins of reefs and the zonation of reef- building organisms. These parameters also play an important role when it comes to the distribution of syndepositional abiotic marine cements in reefs. The variation in leeward and windward margins is documented in the Belize Barrier Reef where abundant syndepositional abiotic marine cementation can be seen on the windward margin (James et al. 1976). Common syndepositional reef cements seen on windward margins include radiaxial fibrous cements, botryoidal cements, and isopachous fibrous High-Mg calcite cements (Flügel, 2004). This variability in the abundance of abiotic marine cements can be applied to the Pipe Creek Jr. reef complex to qualitatively determine the windward and leeward orientation of this reef.

Based upon the samples available for this study, the West Pit is the most pervasively cemented section of the forereef with cements ranging from large void filling botryoidal cements to thick isopachous radiaxial fibrous cements (Tables 2 and 3). High water agitation and large voids allowed for the constant flushing of $CaCO_3$ saturated fluids are key factors needed to precipitate these cements (Flügel, 2004). These parameters are consistent with windward margins of reef settings where the constant flushing of pore spaces due to high wave exposure leads to intensive syndepositional abiotic marine cementation (Flügel, 2004). Trout et al. (2017) documented similar trends to the Pipe Creek Jr. reef complex in a Silurian (Wenlockian) pinnacle reef of the Michigan Basin. In this example, the percentage of syndepositional abiotic marine

cements such as botryoidal cements was highest on the windward margin of the reef and lowest on the leeward margins as previously defined by Wold and Grammer (2017) based upon the facies variability and geometry of the Ray Reef complex. Similar trends were observed in the Late Devonian Iberg reef complex in Germany where syndepositional cements were found to be predominant in the forereef facies on the windward margin of the reef (Webb, 1996). The Tertiary Malampaya and Camago buildups located offshore of the Philippines provide another subsurface example of this windward vs. leeward variability in the distribution of early marine cements. In these buildups extensive cementation that occludes primary porosity occurs on the oceanward (windward) slopes of the buildup due to enhanced water/rock ratios caused by strong swell movements (Grötsch and Mercadier, 1999).

Although the East Pit shows similar cement morphologies as the West Pit, the cements not as prevalent and widespread (Tables 2 and 4). This variation could be related to relatively less agitated waters relative to the interpreted windward margin exposed in the West Pit of the quarry, where higher energy and water circulation likely allowed for more abiotic cement precipitation. The South Pit appears to have mostly syntaxial overgrowth cements (Table 5) and lacks the large (cm-scale) void filling botryoidal and radiaxial fibrous cements typical of windward margins (Grötsch and Mercadier, 1999; Flügel, 2004; Trout et al. 2017; Webb, 1996; Wold and Grammer, 2017). The skeletal grains also appear to be partially to fully micritized. This is a process whereby bioclasts are altered while on the seafloor by endolithic algae, fungi and bacteria that bore around the margins of the skeletal grains (Tucker and Wright, 1990). This micritization can be associated to calmer waters in a less agitated leeward, or oblique to leeward margin of the

reef where there is less current-driven movement of pore fluids (Tucker and Wright, 1990).

Reports on the preservation of steep slope angles by microbial binding in Holocene and Miocene carbonate platforms, and the Silurian example discussed in this study raise the question of whether windward or leeward orientations can be determined by the presence and relative abundance of microbial binding. This criteria, along with the pervasiveness of syndepositional abiotic marine cements can be used to qualitatively determine the orientation of the Pipe Creek Jr. reef complex during deposition. Comparison of the three pits of the Pipe Creek Jr. Quarry (West, East, and South) reveals significant variations in the presence and abundance of the distinct microfabrics indicative of microbial binding. Samples from the West Pit, interpreted as a windward slope based upon the amount of abiotic syndepositional cements, show the largest amount of early microfabrics indicative of early microbial binding, specifically in the form of micrite bridges, trapping and binding dense micrite, and asymmetric micritic crusts (Table 3). The abundance of microbial activity may indicate clear (many of the microbial communities are photosynthetic), nutrient laden waters that would be consistent with good circulation along a windward margin. The East Pit, conversely, has considerably less evidence of microbial binding (Table 4), which is consistent with the lower volumes of syndepositional abiotic marine cements observed, and could be indicative of less well circulated waters along a leeward margin.

Throughout the Silurian, most of Laurentia was in the southeasterly trade wind belt (Spengler and Read, 2010) (Fig. 18A). Based on this paleogepgraphic location, the Illinois Basin (Vincennes Basin) would have been in a leeward position while the Fort

Wayne Bank which borders the Michigan Basin would have been windward (Fig 1B). Individual buildups on the Wabash Platform, however, show a southwest to northeast forereef to backreef polarity which has been suggested by Spengler and Read (201) to be the results of wave driven currents traversing the Illinois Basin from the west and southwest, contrary to the apparent windward/leeward orientation based upon plate reconstruction. These variations in the orientations of the reefs and associated forereef slopes could be the result of local currents induced by other reefs as well as varying sources of normal marine waters through passes and channels (Shaver et al. 1978). This has been suggested for the northern Fort Wayne Bank of the Wabash Platform where Shaver et al. (1978) indicate that later fringing reef growth in this area could have been sourced mostly from the south and west by more normal marine water conditions. This disparity could be the case of the Pipe Creek Jr. reef complex, where based on results from this study, the predominant windward margin or wind direction is from the west (Fig. 19B). It is unclear with the current data set of just one reef and slope complex, but one interpretation would be that the dominant southeasterly winds are responsible for the microbial binding and syndepositional abiotic marine cements seen in the East Pit while waves traversing the Illinois Basin from the west and southwest are a possible explanation for the pervasive syndepositional abiotic marine cements and microbial binding seen in the West Pit. It is also possible that slight revisions to the orientation of the plates relative to the proposed trade winds belts could clarify the argument of the proposed windward vs. leeward variation in the Pipe Creek Jr. reef complex.

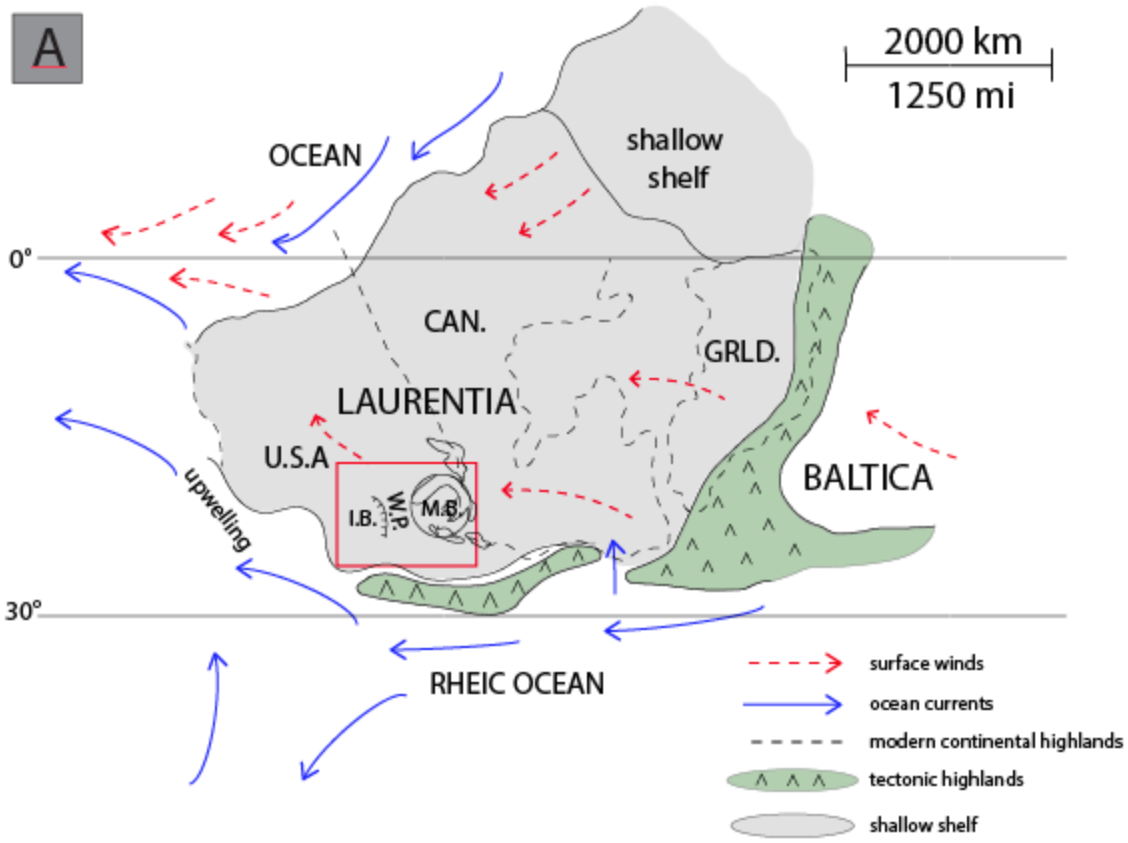
A
2000 km
1250 mi
OCEAN
shallow
shelf
0°
CAN.
GRLD.
LAURENTIA
U.S.A
I.B.
W.P.
M.B.
BALTICA
upwelling
30°
RHEIC OCEAN
surface winds
ocean currents
modern continental highlands
tectonic highlands
shallow shelf

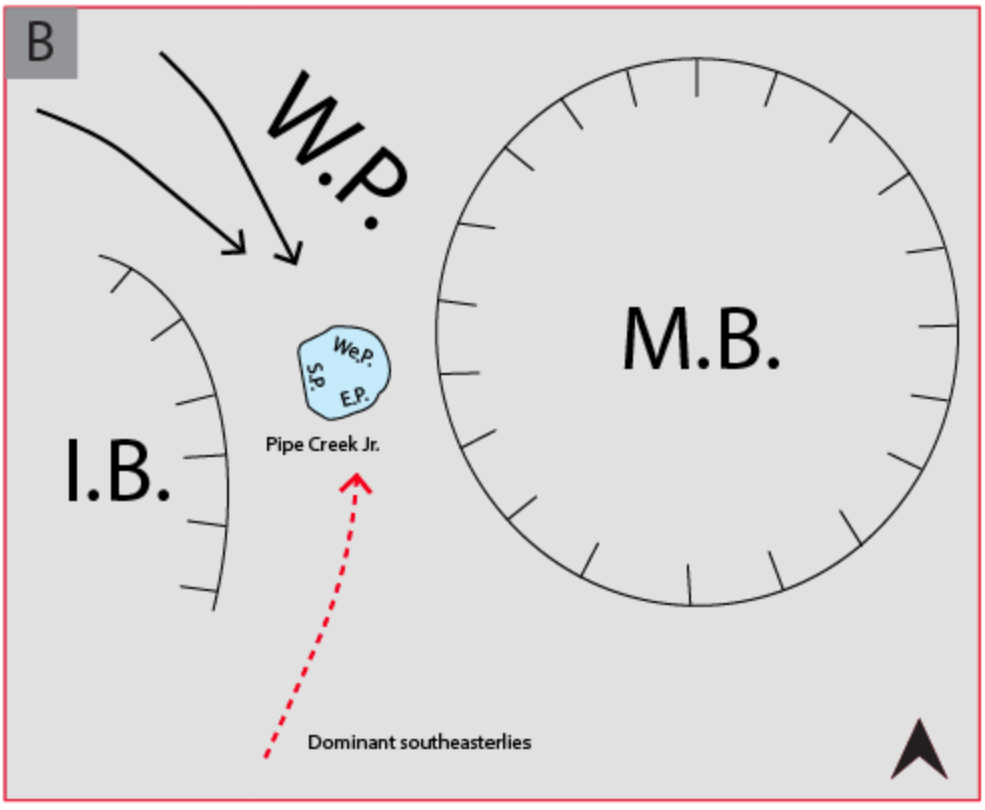
B
W.P.
M.B.
I.B.
We.P.
S.P.
E.P.
Pipe Creek Jr.
Dominant southeasterlies

Figure 18: Late Silurian paleoreconstruction depicting dominant surface winds and ocean currents in relation to the Wabash Platform and the Pipe Creek Jr. reef complex. A) During the Late Silurian southeasterly surface winds dominated (dashed red arrows) in the Wabash Platform (W.P.) and surrounding basins; I.B. is Illinois Basin and M. B. is Michigan Basin (Modified from Spengler and Read, 2010). B) Close up of the Wabash Platform area (W. P.) where dominant southeasterly winds can be seen (dashed red arrow) as well as waves traversing the Illinois Basin from the west and southwest (black arrows). These wind and wave variations are a possible explanation for the deviation in windward vs leeward margins seen at the Pipe Creek Jr. reef complex. The active pits of the Pipe Creek Jr quarry are also denoted: West Pit (We.P.), South Pit (S.P.), and East Pit (E.P.).

Another possibility is that while a well-defined general trend exists showing that windward margins favor reef growth and accretion as well as pervasive syndepositional abiotic marine cementation, there are systems that are exceptions to this pattern. Rankey and Garza-Pérez (2012) examined Holocene atolls in the south Pacific that show better development of reef apron on the southwest facing margin although these lie in the trade-wind belt with dominant winds from the east. This means that the best developed shelf-margin reef and apron is developed on the oblique to leeward side of the atoll and not along the expected windward side. This variability has also been documented on Little Bahama Bank, Crooked–Acklins Platform (Bahamas) and the Caicos Platform (Rankey et al. 2009). Based on these examples, reefs are present on both wave dominated and windward margins (Rankey and Garza-Pérez, 2012) which may or may not be in the same direction/orientation. This variation from the classic windward–leeward model could be another explanation for the disparity seen at the Pipe Creek Jr. reef complex between the proposed windward orientation based on this work and the reported predominant wind direction during the Late Silurian.

# CHAPTER V

## SUMMARY AND CONCLUSIONS

The influence of microbial carbonates and microbial binding is well documented in numerous modern and Cenozoic examples of steep carbonate slope deposits. Nevertheless its significance and relationship with abiotic marine cements in ancient steep carbonate slope deposits and ancient reef systems has not yet been fully determined or understood. This work addressed this subject by studying the influence of these diagenetic processes in steep (35-45°) Silurian (Cayugan) forereef slope deposits exposed at the Pipe Creek Jr. Quarry (IN).

This work addressed several primary objectives:

1. Document the presence of microbial binding in the steep Silurian forereef slope deposits at the Pipe Creek Jr. quarry:

   This work shows that there is presence of microbial binding in these deposits. Distinct microfabrics indicative of microbial binding were identified in thin sections of these deposits. Furthermore, SEM analysis identified fossilized bacterial communities and bacterial biofilms. Although the presence of bacteria-like structures and EPS support a microbial origin for the microfabrics observed

in samples from the Pipe Creek Jr. reef complex, other later stage fluids such as hydrocarbon emplacement may be responsible for the presence of some of these features.

2. Evaluate the contribution of microbial binding to the stabilization and lithification of these deposits:

    Microbial binding of sediment in the forereef slopes of the Pipe Creek Jr. reef complex is proposed as an early stage stabilizing and lithifying agent. This microbial binding inhibits slope failure and conserves the steep angles of the forereef slopes. Microfabrics that show early lithification include dense micrite bridges which allow the preservation of open pore space that was occluded by later abiotic marine cements. Various reefs and slope examples including the Holocene TOTO (Bahamas), upper Miocene Cariatiz platform (Spain), the Middle and Upper Capitan Formations of the Permian Capitan reef, Late Miocene *Halimeda* alga-microbial segment reefs in the Sorbas Basin (Spain), and the Tengiz Field of the Precaspian Basin (Kazakhstan) contain similar microfabrics.

3. Determine a paragenetic relationship between microbial binding and abiotic marine cements:

    Stabilization by microbial binding essentially occurs before the stabilization by abiotic marine cements which have been shown to precipitate syndepositionally (some within the first hundreds of years after deposition) and at rates faster than the 8-10 mm/yr as reported by Grammer et al. (1993b). A clear paragenetic relationship was identified through petrographic analysis which

further confirms that microbial binding precedes additional stabilization by syndepositional abiotic marine cements. Microbial binding creates a stable substrate that aids in the later precipitation of syndepositional abiotic marine cements. Although petrographic analysis demonstrates this relationship, SEM analysis fails to capture this paragenetic relationship in an unequivocal manner.

4. Evaluate whether there is a windward vs. leeward orientation of the reef complex based on the relative amounts and distribution of microbial binding and syndepositional abiotic marine cements in the different locations (West, East, and South) of the quarry:

Windward and leeward orientations of the Pipe Creek Jr. reef complex were determined by the relative abundance of syndepositional abiotic marine cements and microbial binding. Comparison of the relative abundance of microbial binding and morphologies of syndepositional abiotic marine cements in the three pits of the Pipe Creek Jr. Quarry (West, East, and South) reveals variations due to interpreted windward and leeward orientations of the Pipe Creek Jr. reef complex. Based on this work, the West Pit appears to be the most pervasively cemented section of the reef and is interpreted as likely being in a windward margin facing location. The East Pit shows similar cement morphologies and microfabrics of microbial binding as the West Pit but neither are as prevalent and widespread as observed in the West Pit. This can be interpreted as relatively less agitated waters in the East Pit than in the West Pit yet not calm enough to be considered the leeward margin. The South Pit is considered to be in the most leeward margin position of the reef as it is mostly characterized

by syntaxial overgrowth cements and lacks large (cm-scale) void filling botryoidal and radiaxial fibrous cements typically found in windward margins.

Uncertainties presented in previous studies of Cayugan-aged reefs in the region suggest that the paleogeographic location and orientation of the Pipe Creek Jr. reef and forereef slope complex may have been oriented more oblique to postulated trade wind belts. Additionally, some studies suggest the combination of a primary wind driven wave regime that is separate and oriented differently from other marine currents. Although there is a strong suggestion regarding the windward and leeward slopes of the Pipe Creek Jr. complex based upon facies types and bed geometries (Karsten, in progress), and the amount of abiotic and microbial cementation reported in this study, the exact positioning of the Pipe Creek Jr. reef and slope complex is difficult to ascertain from this one example. As such, further work on multiple reefs and reef complexes in this region is necessary to further evaluate the paleogeographic and paleoceanographic conditions of this area during the Silurian.

# CHAPTER VI

## SUGGESTIONS FOR ADDITIONAL RESEARCH

This study served to further discussions on the role of microbial communities in microbial binding and biotic cementation in reef systems as well as in steep carbonate slopes throughout geologic history. Further research on the Pipe Creek Jr. reef complex, as well as the study of a modern reef analog, could provide new insights into microbial processes (metabolic and calcifying processes) and microbial communities that could strengthen the conclusions made in this work. Some of the questions and discussions that have resulted from this study include:

1) *Textural bias?*

Hand samples available for this work were mostly higher energy skeletal packstones-grainstones, likely from the middle to upper portions of the forereef slopes. These samples showed abundant microfabrics indicative of microbial binding as discussed herein. This sampling and textural bias raises the question of whether there is microbial binding and cementation occurring in lower energy environments such as the toe of slope. If so, could there be a difference in the microfabrics observed in higher energy settings than those from lower energy settings? Could this difference be related to distinct microbial communities in each setting? Continuous cores taken a few meters behind current wall exposures

that samples both the skeletal packstones-grainstones as well as the thinner mudstones-wackestones could aid in answering this question.

*Deep vs. shallow?*

The photic zone is often discussed as being in the range of 40-60 m deep. Recent studies on Holocene reef systems and carbonate slopes, however, have shown this to be highly variable dependent upon water clarity. The presence of green and red algae in the Tongue of the Ocean (Bahamas) at depths of up 150 m suggests that photosynthetic organisms can still thrive at depths below what is often considered as the limit of the photic zone (Grammer et al. 1993a). This raises the question of whether the microbial communities documented at the Pipe Creek Jr. reef complex were purely photosynthetic or not. Could there be distinct microfabrics produced by photosynthetic microbial communities vs. non-photosynthetic (e.g. sulfate reducing) bacteria? Would it be possible to sample toe of slope units to make this comparison either with continuous core behind the quarry walls, or possibly moving out (i.e. more distal) from the reef complex?

2) *Dolomite?*

The presence of dolomite at the Pipe Creek Jr. reef complex is minor when compared to nearby reefs that have undergone significant dolomitization. At the Pipe Creek Jr. reef complex, dolomite is seen as silt sized subhedral to euhedral crystals that form thin lenses sporadically throughout the exposed forereef slopes. The reason as to why dolomitization was not pervasive at the Pipe Creek Jr. reef complex still remains unanswered. Studies have suggested that the pervasive

abiotic marine cementation reduced available porosity which prevented dolomitizing fluids to migrate through the system. The origin and timing of this dolomite also remains unclear. There is no evidence observed for hydrothermal origin and although there is some evidence that supports evaporitic conditions and subsequent “top-down” early dolomitization up section of the reef complex, these evaporites were not observed at the Pipe Creek Jr. reef complex. Therefore the origin and timing of dolomite still remains unanswered. Further geochemical work and possibly structural and tectonic study may aid in answering this question.

# REFERENCES


BACELLE, L., AND BOSELLINI, A., 1965, Diagrammi per la stima visive della composizione percentuale nelle rocche sedimentarie, Annali dell'Università di Ferrara (Nuova Serie), Sezione 9, Scienze geologinche e paleontologiche, vo. 1, no. 3, p. 59-62.

BATHURST, R. G. C., 1975, Carbonate Sediments and their Diagenesis, Developments in Sedimentology 12, 2nd Ed.: Elsevier, Amsterdam, 658 p.

BEERBOWER, D.C., 1977, Relationship between clay and dolomitization in the Pipe Creek Jr. Reef (Silurian), Grant County, Indiana [unpublished M.S. thesis]: Ball State University, 57 p.

BRACHERT, T. C., AND DULLO, W. C., 1989, Laminar Micrite Crusts and Associated Foreslope Processes, Red Sea: Journal of Sedimentary Petrology, v. 61, no. 3, p. 354-363

BOURQUE, P. –A., 1998, Silurian reefs, *in* Geldsetzer, H. H. J., James, N. P. and Tebbutt, G. E., eds., Reefs, Canada and Adjacent Areas: Memoir, Canadian Society of Petroleum Geologists, v. 13, p. 245-250.

BUCZYNKSI, C., AND CHAFETZ, H.S., 1991, Habit of Bacterially Induced Precipitates of Calcium Carbonate and the Influence of Medium Viscosity of Mineralogy, Journal of Sedimentary Petrology, v. 61, no. 2, p. 226-233.

COLLINS, J. F., KENTER, J. A. M., HARRIS, P. M., KUANYSHEVA, G., FISCHER, D. J., AND STEFFEN, K. L., 2006, Facies and reservoir-quality variations in the late Visean to Bashkirian outer platform, rim, and flank of the Tengiz buildup, Precaspian Basin, Kazakhstan, *in* P. M. Harris and L. J. Weber, eds., Giant hydrocarbon reservoirs of the world: From rocks to reservoir characterization and modeling: AAPG Memoir 88/SEPM Special Publication, No. p. 55-95.

DARWIN, C.R., 1842, Structure and Distribution of Coral Reefs: Smith Elder, London, 214 p.

DELLA PORTA, G., KENTER, J.A.M., BAHAMONDE, J.R., IMMENHAUSER, A., AND VILLA, E., 2003, Microbial boundstone dominated carbonate slope (Upper Carboniferous, N Spain): microfacies, lithofacies distribution and stratal geometry: Facies, v. 49, p. 175–208.

DELLA PORTA, G., MERINO-TOMÉ, O., KENTER, J.A.M., AND VERWER, K., 2013, Lower Jurassic microbial and skeletal carbonate factories and platform geometry (Djebel Bou Dahar, High Atlas, Morocco), *in* Verwer, K., Playton, T.E., and Harris, P.M., eds., Deposits, Architecture, and Controls of Carbonate Margin, Slope, and Basinal Settings: SEPM, Special Publication 105, p. 237–263.

DEVANEY, K.A., WILKINSON, B.H., AND VAN DER VOO, R., 1986, Deposition and compaction of carbonate clinothems: The Silurian Pipe Creek Junior Complex of east-central Indiana: Geological Society of America, Bulletin, v. 97, p. 1367–1381.

DIAZ, M. R., EBERLI, G. P., BLACKWELDER, P., PHILLIPS, B., AND SWART, P. K., 2017, Microbially mediated organomineralization in the formation of ooids: GEOLOGY, v. 45, no. 9, p. 771-774.

DUNHAM, R. J., 1962, Classification of carbonate rocks according to depositional texture: AAPG Memoir v. 1, p 108-121.

ENOS, P., 1977, Tamabra Limestone of the Poza Rica Trend, Cretaceous, Mexico, in Cook, H.E., and Enos. P., eds., Deep-Water Carbonate Environments: SEPM, Special Publication 25, p. 273–314.

FLEMING, A. H., FARLOW, J. O., ARGAST, A., GRAMMER, G. M., AND PREZBINDOWSKI, D., 2018, The Maumee Megaflood and the geomorphology, environmental geology, and Silurian-Holocene history of the upper Wabash Valley and vicinity, north- central Indiana, in Florea, L. J., ed., Ancient Oceans, Orogenic Uplifts, and Glacial Ice: Geologic Crossroads in America's Heartland: Geological Society of America Field Guide 51. P. 259-337.

FLÜGEL, E., 2004, Microfacies of Carbonate Rocks- Analysis, Interpretation and Application: Springer, London, New York, 984 p.

FRANK, T. D., WILKINSON, B. H., AND LOHMANN, K., 1993, Origin of submarine pisoliths and the sedimentology of Midwestern Silurian reefs, Journal of Sedimentary Research, v. 63, no. 6, p. 1070-1077.

FOLK, R., 1993, SEM Imaging of Bacteria and Nanobacteria in Carbonate Sediments and Rocks, Journal of Sedimentary Petrology, v. 63, no. 5, p. 990-999.

GEBHARDT, L. P., AND ANDERSON, D. A., 1954, Microbiology: The C.V. Mosby Company, St. Louis, 413 p.

GISCHLER, E., 1995, Current and Wind Induced Facies Patterns in a Devonian Atoll: Iberg Reef, Harz Mts, Germany: PALAIOS, v. 10, no. 2, p. 180-189.

GODDARD, E.N., TRASK, P. D., DE FORD, R. K., ROVE, O. N., SINGEWALD, J. T., OVERBECK, R. M., 1970, Rock Color Chart, The Geological Society of America: Boulder, Colorado.

GRAMMER, G. M., GINSBURG, R., AND HARRIS, P. M., 1993a, Timing of Deposition, Diagenesis, and Failure of Steep Carbonate Slopes in Response to a High-Amplitude/High-Frequency Fluctuation in Sea Level, Tongue of the Ocean, Bahamas, in R. Loucks, J. F. Sarg, eds., Carbonate Sequence Stratigraphy: Recent Developments and Applications, AAPG Memoir v. 57, p. 107-131.

GRAMMER, G. M., GINSBURG, R., SWART, P., MCNEILL, D., JULL, A., AND, Prezbindowski, D., 1993b, Rapid Growth Rates of Syndepositional Marine Aragonite Cements in Steep Marginal Slope Deposits, Bahamas and Belize: Journal of Sedimentary Petrology, v. 63, p. 983-989.

GRÖTSCH, J., AND MERCADIER, C., 1999, Integrated 3-D Reservoir Modeling Based on 3-D Seismic: Tertiary Malampaya and Camago Buildups, Offshore Palawan, Philippines: AAPG Bulletin, v. 83, no. 11, p. 1703-1728.

HADDAD, A., AISSAOUI, M.D., AND SOLIMAN, M.A., 1984, Mixed carbonate–siliciclastic sedimentation on a Miocene fault-block, Gulf of Suez: Sedimentary Geology, v. 37, p. 182–202.

HARRIS, M. T., 1993, Reef fabrics, biotic crusts and syndepositional cements of the Latemar reef margin (Middle Triassic), Northern Italy: Sedimentology, v. 40, p. 383-401.

HARRIS, P. M., DIAZ, M. R., AND EBERLI, G. P., 2019, The Formation and Distribution of Modern Ooids on Great Bahama Bank, Annual Review of Marine Science, v. 11, p. 491-516.

JAMES, N.P., GINSBURG, R.N., MARSZALEK, D.S., AND CHOQUETTE, P.W., 1976, Facies and fabric specificity in early subsea cements in shallow Belize (British Honduras) reefs: Journal of Sedimentary Petrology, v. 46, p. 523-544.

KEIM, L., AND SCHLAGER, W., 1999, Automicrite facies on steep slopes (Triassic, Dolomites, Italy): Facies, v. 41, p. 15–25.

KENTER, J.A.M., HARRIS, P.M., AND DELLA PORTA, G., 2005, Steep microbial boundstone dominated platform margins: examples and implications: Sedimentary Geology, v. 178, p. 5–30.

KIRKLAND, B. L., DICKSON, J. A. D., WOOD, R. A., AND LAND, L. S., 1998, Microbialite and Microstratigraphy: the Origin of Encrustations in the Middle and Upper Capitan Formation, Guadalupe Mountains, Texas and New Mexico, U.S.A, Journal of Sedimentary Research, v. 68, No. 5, p. 956-969.

LEHMANN, P.J., 1978, Deposition, porosity evolution and diagenesis of the Pipe Creek Jr. Reef (Silurian), Grant County, Indiana [unpublished M.S. thesis]: Department of Geology and Geophysics, University of Wisconsin–Madison, 234 p.

LEHMANN, P. AND SIMO, J., 1988, Depositional Facies and Diagenesis of the Pipe Creek Jr. Reef, Silurian, Great Lakes Region, Indiana, CSPG Special Publication, Memoir 13, p. 319-329.

LOHMANN, K.C., 1988, Geochemical patterns of meteoric diagenesis systems and their application to studies of paleokarst, in James, N.P., and Choquette, P.W., eds., Paleokarst: Berlin, Springer-Verlag, p. 58–80.

MARTÍN, J.M., BRAGA, J.C., AND RIDING, R., 1997, Late Miocene Halimeda alga–microbial segments reefs in the marginal Mediterranean Sorbas Basin, Spain: Sedimentology, v. 44, p. 441–456.

MOORE, C.H., 2001, Carbonate Reservoirs: Porosity, Evolution and Diagenesis in a Sequence Stratigraphic Framework, Developments in Sedimentology, v. 55, p. 93-144.

RANKEY, E. C., AND GARZA-PÉREZ, J. R., 2012, Seascape Metrics of Shelf-Margin Reefs and Reef Sand Aprons of Holocene Carbonate Platforms: Journal of Sedimentary Research, v. 82, p. 57-75.

RANKEY, E. C., GUIDRY, S. A., REEDER, S. L., AND GUARIN, H., 2009, Geomorphic and sedimentologic heterogeneity along a Holocene shelf margin, Caicos Platform: Journal of Sedimentary Research, v. 79, p. 440-456.

REEDER, R. J., AND PAQUETTE, J., 1989, Sectoral zoning in natural and synthetic calcites: Sedimentary Geology, v. 65, p. 239-247.

REID, R.P., MACINTYRE, I. G., AND JAMES, N. P., 1990, Internal Precipitation of Microcrystalline Carbonate: a Fundamental Problem for Sedimentologists, Sedimentary Geology, v. 68, p. 163-170.

REOLID, J., BETZLER, C., BRAGA, J.C., MART´IN, J.M., LINDHORST, S., AND REIJMER, J.G., 2014, Reef slope geometries and facies distribution: controlling factors (Messinian, SE Spain): Facies, v. 60, p. 737–753.

REOLID, J., BETZLER, C., EBERLI, G. P., AND GRAMMER, G. M., 2017, The Importance of Microbial Binding in Neogene–Quaternary Steep Slopes: Journal of Sedimentary Research, v. 87, p. 567-577.

RIDING, R., 2000, Microbial carbonates: the geological record of calcified bacterial-algal mats and biofilms: Sedimentology, v. 47, p. 179-214.

RIDING, R., 1991, Classification of Microbial Carbonates, *in* Riding R., eds., Calcareous Algae and Stromatolites: Springer, Berlin, p. 21-51.

ROMANIN, M., CRIPPA, G., YE, F., BRAND, U., BITNER, M. A., GASPARD, D., HÄUSSERMANN, V., AND LAUDIEN, J., 2018, A Sampling Strategy for Recent and Fossil Brachiopods: Selecting the Optimal Shell Segment for Geochemical Analyses, Rivista Italiana de Paleontologia e Stratigrafia, v. 124, p. 343-359

SCHLAGER, W., 1981, The paradox of drowned reefs and carbonate platforms: Geological Society of America, Bulletin, v. 92, p. 197–211.

SCHLAGER, W., AND CAMBER, O., 1986, Submarine slope angles, drowning unconformities, and self-erosion of limestone escarpments: Geology, v. 14, p. 762–765.

SCHOLLE, P.A, AND ULMER-SCHOLLE, D.S., 2003, A Color Guide to the Petrography of Carbonate Rocks: Grains, Textures, Porosity, Diagenesis, AAPG Memoir 77, Tulsa, OK, U.S.A., 474p.

SHAVER, R.H., AULT, C.H., AUSICH, W.I., DROSTE, J.B., HOROWITZ, A.S., JAMES, W.C., OKLA, S.M., REXROAD, C.B., SUCHOMEL, D.M., WELCH, J.R., 1978. The Search for a Silurian Reef Model; Great Lakes Area. Special Report — Indiana, Geological Survey. 36 p.

SHAVER, R. B. AND, SUNDERMAN, J. A., 1989, Silurian seascapes: Water depth, clinothems, reef geometry, and other motifs- A critical review of the Silurian reef model: Geological Society of America Bulletin, v. 101, p. 939-951.

SIMO, J., & LEHMANN, P. J., 2000, Diagenetic History of Pipe Creek Jr. Reef, Silurian, North-Central Indiana, U.S.A.: Journal of Sedimentary Research, v. 70, no. 4, p. 937-951.

SPENGLER, A. E., AND J.F. READ, 2010, Sequence development on a sediment-starved, low accommodation epeiric carbonate ramp: Silurian Wabash Platform, USA mid-continent during icehouse to greenhouse transition: Sedimentary Geology, v. 224, p. 84-115.

SUCHOMEL, D.M., 1975, Paleoecology and petrology of Pipe Creek Jr. Reef (Niagaran–Cayugan), Grant County, Indiana [unpublished M.A. thesis]: Indiana University–Bloomington, 38 p.

SUNDERMAN, J.A., AND MATHEWS, G.F., 1975, Age and origin of clastic dikes in Silurian reefs of northern Indiana: Society of Economic Petrologists and Mineralogists, Great Lake Section, 5th Annual Field Conference, p. 72–83.

TRICHET, J., AND DÉFARGE, C., 1995. Non-biologically supported organomineralization: Bulletin de l'Institut Océanographique (Monaco) Numéro Spécial 14, p. 203–236.

TROUT, J.L., GRAMMER, G.M., AND HARRISON, W.B., III, 2017, Windward vs. leeward variability of faunal distribution in a Silurian (Wenlockian) pinnacle reef complex—Ray Reef, Macomb County, Michigan, *in* Grammer, G.M., Harrison, W.B., III, and Barnes, D.A.,eds., Paleozoic Stratigraphy and Resources of the Michigan Basin: Geological Society of America Special Paper 531, p. 1–25.

TUCKER, M. E., AND, WRIGHT, V. P., 1990, Carbonate Sedimentology: Blackwell Science Ltd., Oxford, UK, 481 p.

WEBB, G. E., 1996, Was Phanerozoic reef history controlled by the distribution of non-enzymatically secreted reef carbonates? (microbial carbonate and biologically induced cement)?: Sedimentology v. 43, p. 947-971.

WENZEL, B., AND JOACHIMSKI, M.M., 1996, Carbon and oxygen isotopic composition of Silurian brachiopods (Gotland/Sweden): palaeoceanographic implications: Palaeogeography, Palaeoclimatology, Palaeocology, v. 122, p. 143–166.

WESTALL, F., DE WIT, M. J., DANN, J., VANDER GAAST, S., DE RONDE, C. E. J., AND GERNEKE, D., 2001, Early Archean fossil bacteria and biofilms in hydrothermally-influenced sediments from the Barberton greenstone belt, South Africa, Precambrian Research v. 106, p. 93-116.

WOLD, J. L., and Grammer, G.M, 2017, Rock-based 3-D reservoir characterization of a Silurian (Niagaran) reef- Ray gas storage field, Macomb County, Michigan, *in* Grammer, G.M., Harrison, W.B., III, and Barnes, D.A., eds., Paleozoic Stratigraphy and Resources of the Michigan Basin: Geological Society of America Special Paper 531, p. 105-129.

WOLICKA, D., AND BORKOWSKI, A., 2012, Microorganisms and Crude Oil, *in* Romero-Zerón, L., eds., Introduction to Enhanced Oil Recovery (EOR) Processes and Bioremediation of Oil- Contaminated Sites: IntechOpen, p. 113-142.

# APPENDICES

*West Pit Results*

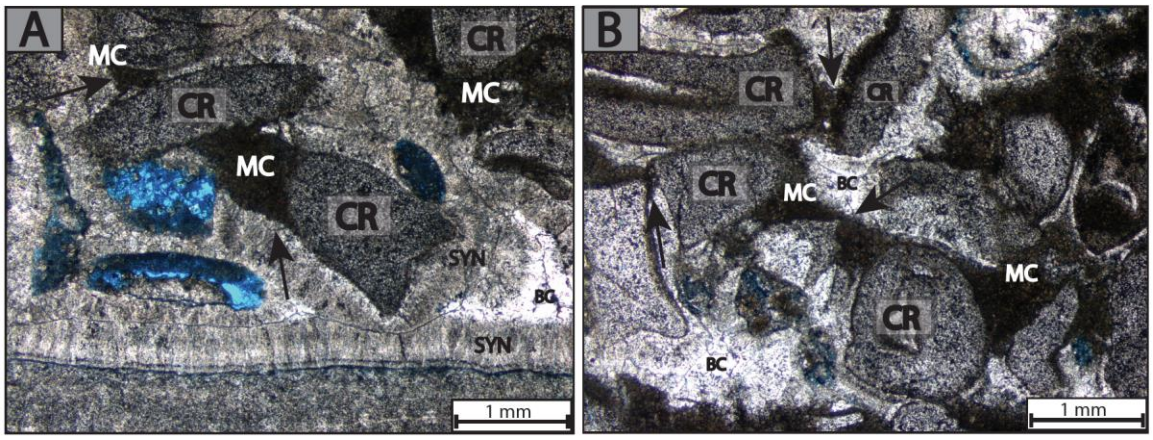


Figure A1: Photomicrographs of the dense micrite in samples collected from the West Pit of the Pipe Creek Jr. Quarry: A-B) Micritic bridge-like structures (black arrows/MC) can bind various crinoid grains (CR). This micrite shows early lithification by preserving initial porosity that was occluded by later abiotic marine cements which include blocky calcite cements (BC).

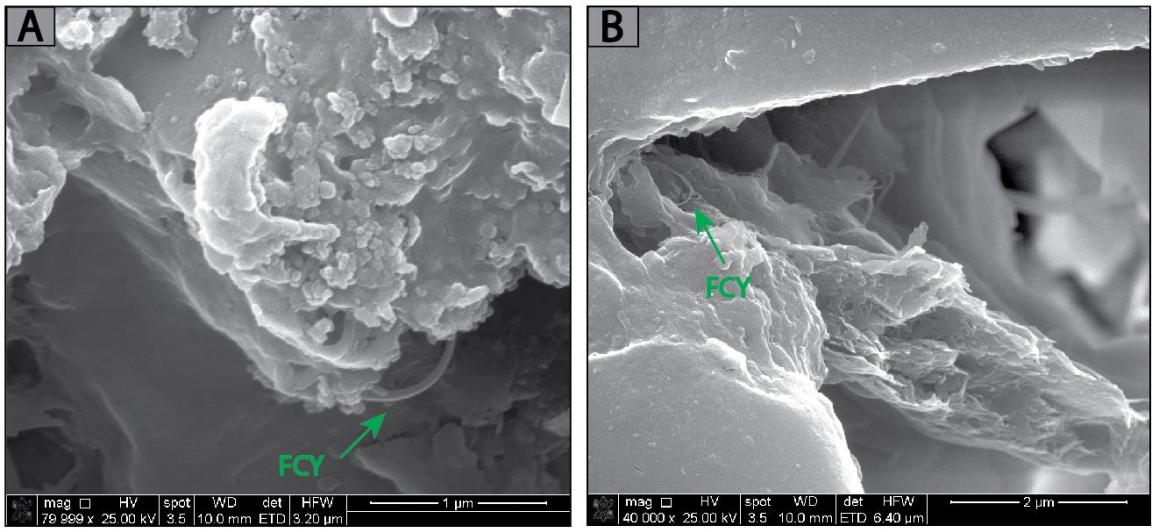


Figure A2: SEM images of ion-milled samples of the forereef slope deposits: A) Green arrows depict filamentous cyanobacteria fossils (FCY), some of which are slightly curved. This FCY is seen in association with nanograin clusters. Scale bar is 1 micron; Scale bar is 2 micron.

*East Pit Results*

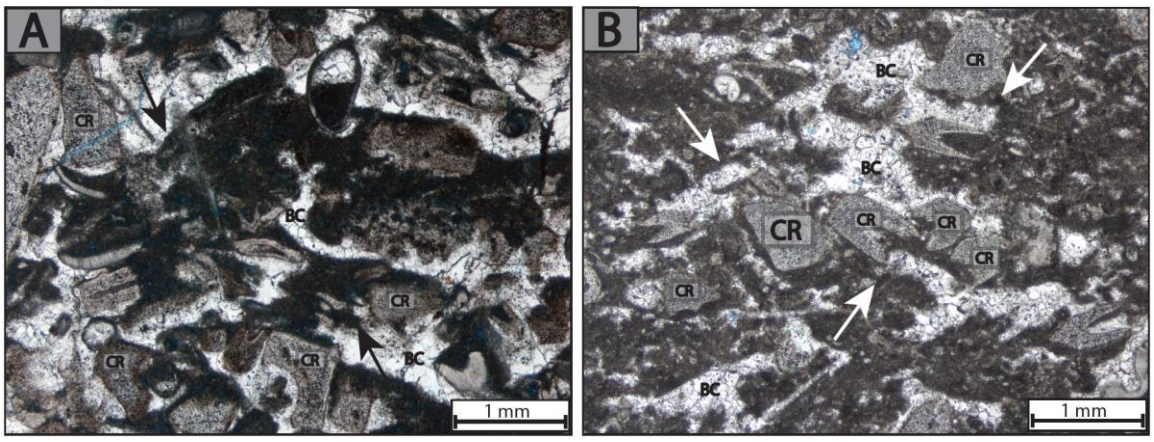


Figure A3: Photomicrographs of the dense micrite in samples collected from the East Pit of the Pipe Creek Jr. Quarry: A) Micrite bridges of dense micrite (black arrows/MC) locally connect crinoid grains (CR). Preferential precipitation appears on the upper part of the sample (notice geopetal structure). B) Micrite bridges (white arrows) appear somewhat peloidal and laminated and can preserve some of the original porosity which was occluded by abiotic marine cements (BC).

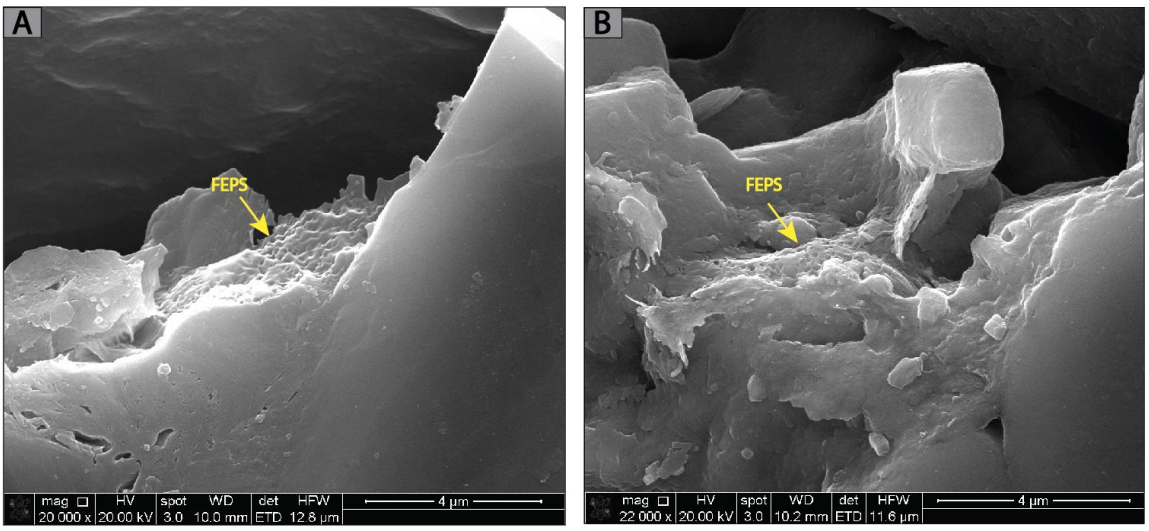


Figure A4: SEM images of ion-milled samples of the forereef slope deposits from the East Pit: A-B) Mucus like FEPS can be seen lining remaining porosity (yellow arrows). Scale bar is 4 microns on both images.

*Energy Dispersive X-Ray Spectroscopy Results*

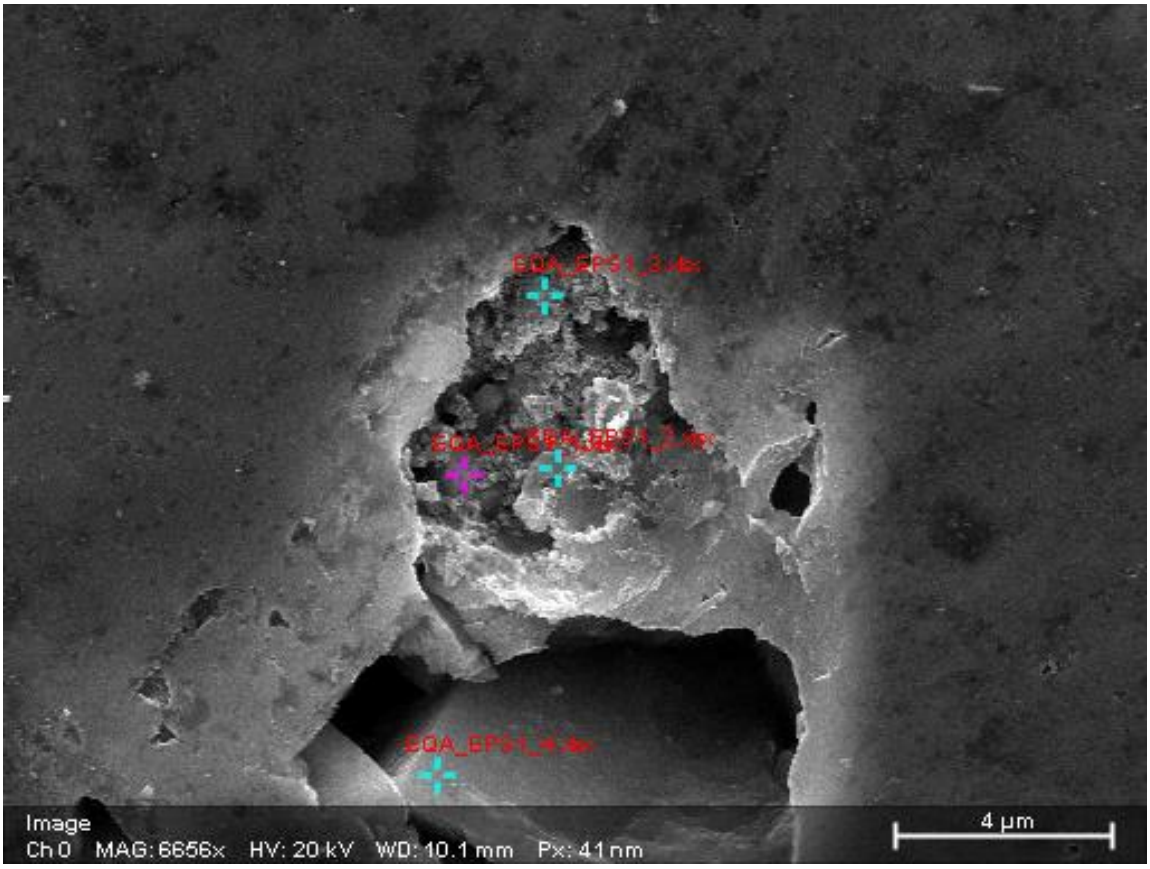


Figure A5: SEM images of ion-milled samples of the forereef slope deposits from the East Pit (refer to Fig. 13A) of fossilized extracellular polymeric substances (FEPS) in association with a cluster of nanograin structures within remaining porosity. Measured points are labelled in red (1-4) which include interpreted EPS (1-3), and calcite grains (4).

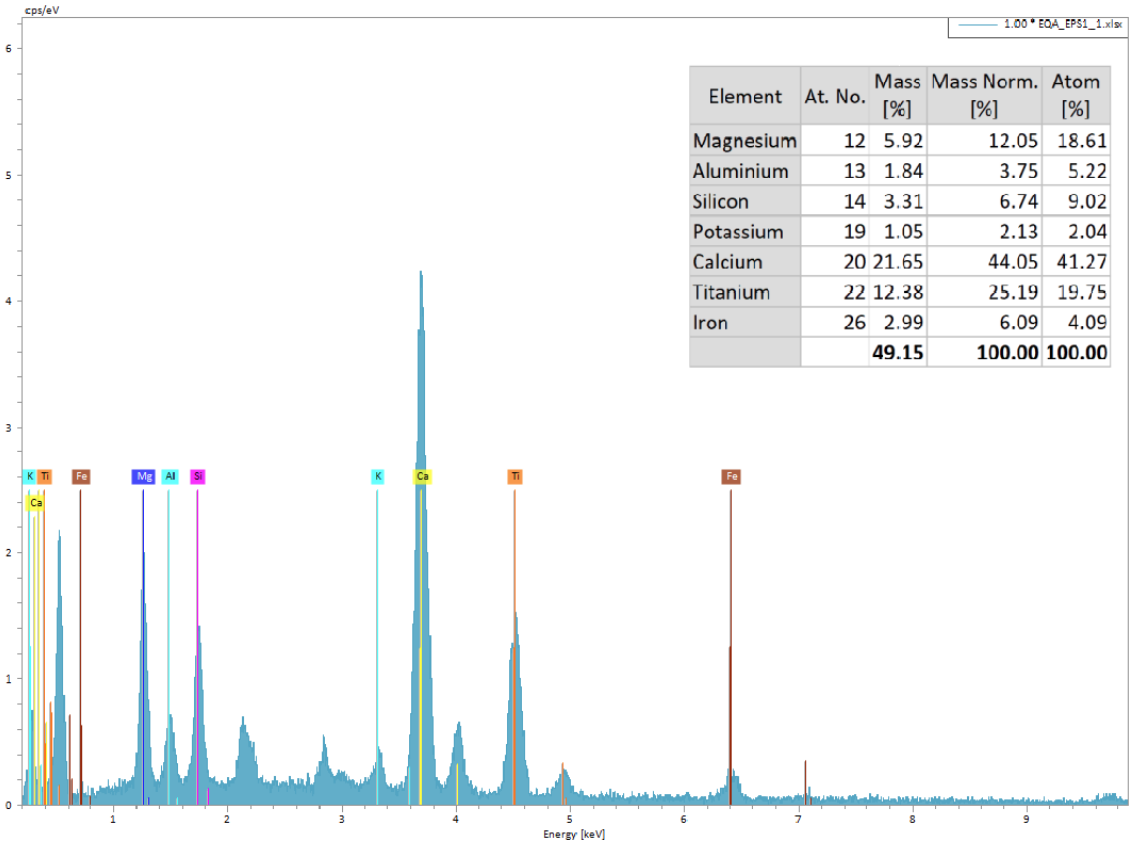


Figure A6: EDS spectra for point 1 (FEPS) seen in Fig. A5. Elemental composition of the analyzed point shows normalized mass of 44.05% calcium (Ca), 25.19% titanium (Ti), 12.05% magnesium (Mg), 6.74% silicon (Si), 6.09% iron (Fe), 3.75% aluminium (Al), and 2.13% potassium (K). The large mass percentage of calcium further confirms the interpretation of FEPS.

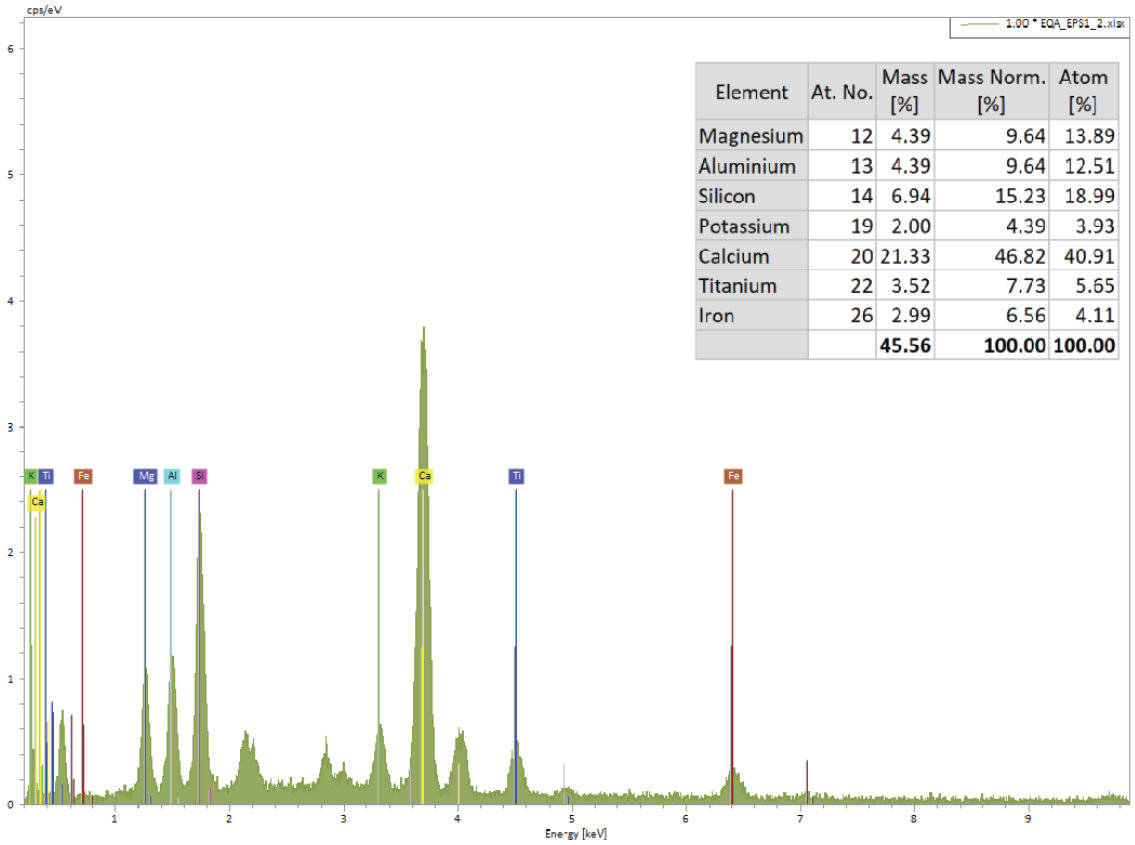


Figure A7: EDS spectra for point 2 (FEPS) seen in Fig. A5. Elemental composition of the analyzed point shows normalized mass of 46.82% calcium (Ca), 15.23% silicon (Si), 9.64% of magnesium (Mg) and aluminium (Al), 7.73% titanium (Ti), 6.56% iron (Fe), and 4.39% potassium (K). The large mass percentage of calcium further confirms the interpretation of FEPS.

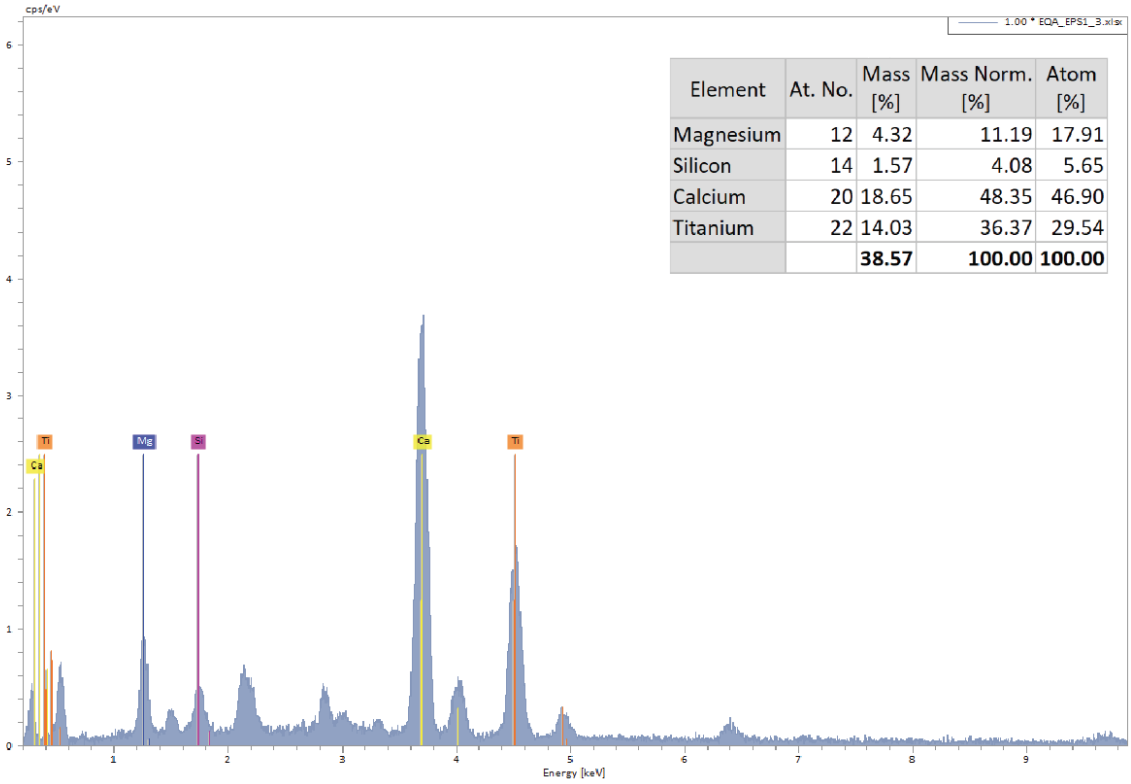


Figure A8: EDS spectra for point 3 (FEPS) seen in Fig. A5. Elemental composition of the analyzed point shows normalized mass of 48.35% calcium (Ca), 36.37% titanium (Ti), 11.19% magnesium (Mg), and 4.08% silicon (Si). The large mass percentage of calcium further confirms the interpretation of FEPS.

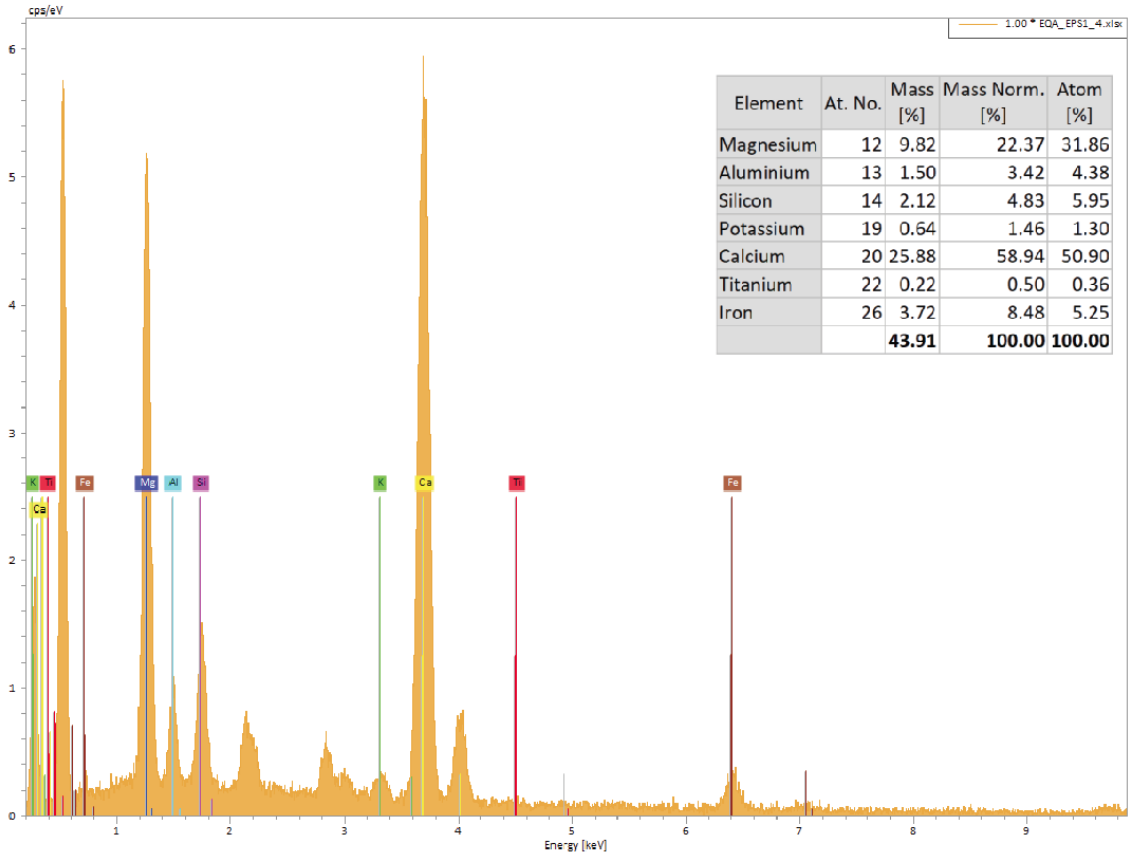


Figure A9: EDS spectra for point 4 (calcite crystal) seen in Fig. A5. Elemental composition of the analyzed point shows normalized mass of 58.94% calcium (Ca), 22.37 magnesium (Mg), 8.48% iron (Fe), 4.83% silicon (Si), 3.42% aluminium (Al), 1.46% potassium (K), and 0.50% titanium (Ti).

*South Pit Results*

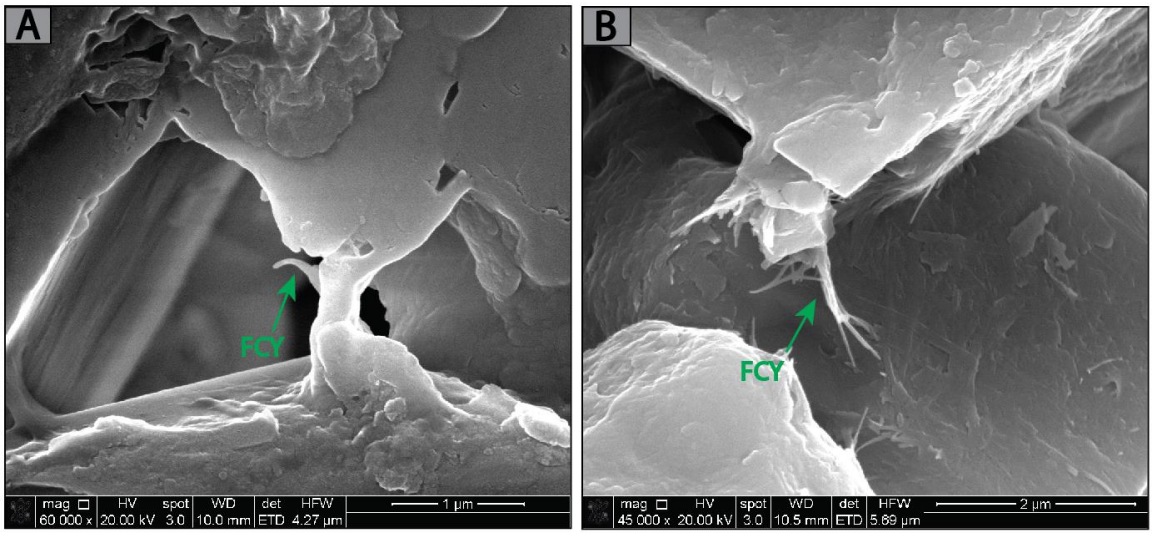


Figure A10: SEM images of ion-milled samples of the forereef slope deposits: A) Green arrows depict filamentous cyanobacteria fossils (FCY), some of which are slightly curved. B) A cluster of what appears to be FCY can be seen protruding from a calcite crystal. Scale bar is 1 micron; Scale bar is 2 micron.

*Energy Dispersive X-Ray Spectroscopy Results*

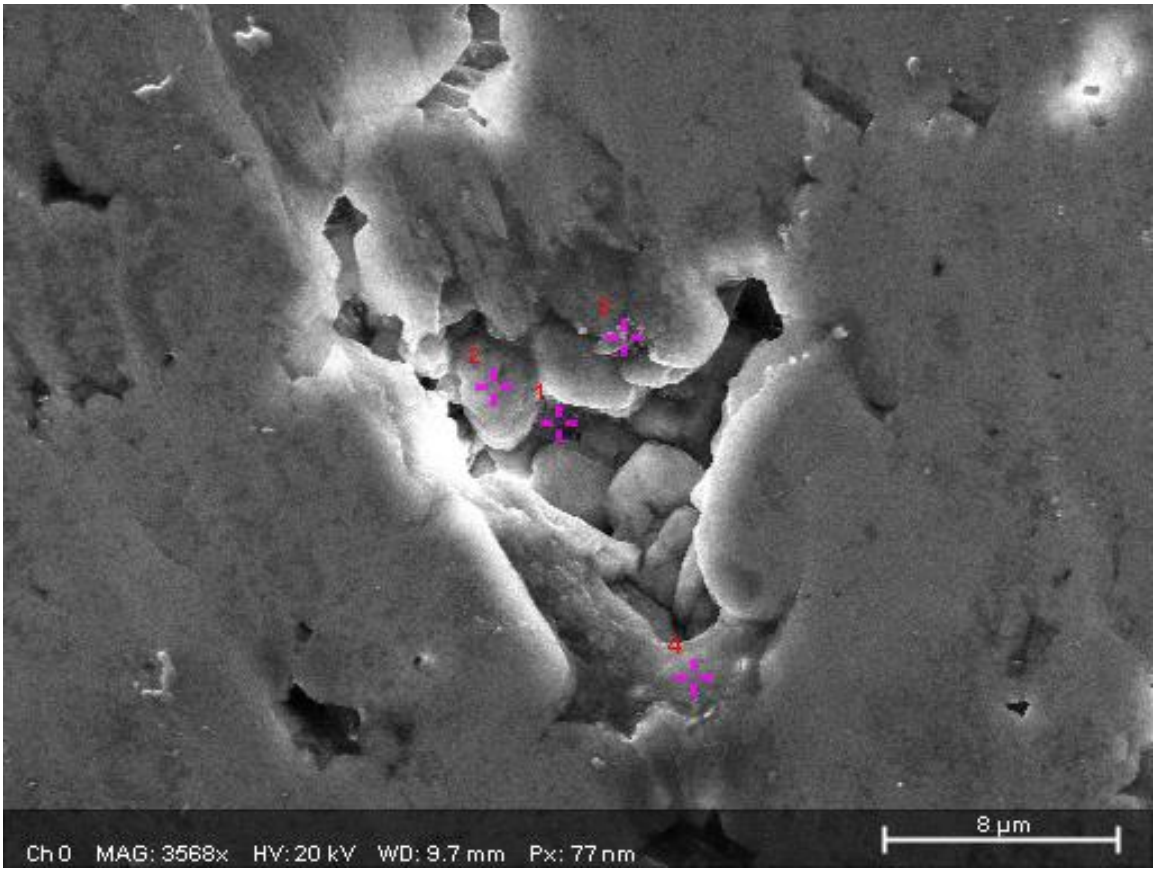


Figure A11: Figure A5: SEM images of ion-milled samples of the forereef slope deposits from the South Pit (refer to Fig. 15B) of fossilized extracellular polymeric substances (FEPS) which has a honeycomb-like appearance. This FEPS is seen at grain contacts and in association with a cluster of nanograins. Measured points are labelled in red (1-4) which include interpreted EPS (1), calcite grains (2-3), and pore surface (4).

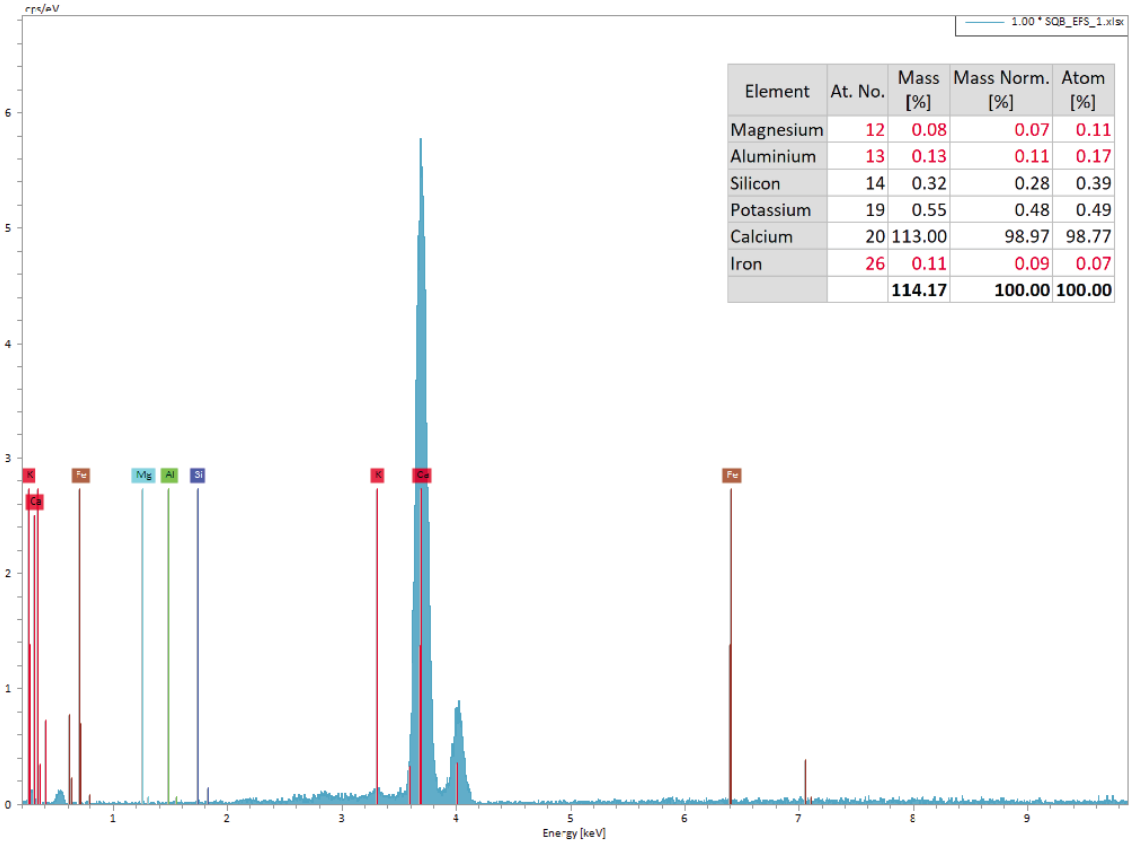


Figure A12: EDS spectra for point 1 (FEPS) seen in Fig. A10. Elemental composition of the analyzed point shows normalized mass of 98.97% calcium (Ca), 0.48% potassium (K), 0.28% silicon (Si), 0.11% aluminium (Al), 0.09% iron (Fe), and 0.07% magnesium (Mg). The large mass percentage of calcium further confirms the interpretation of FEPS.

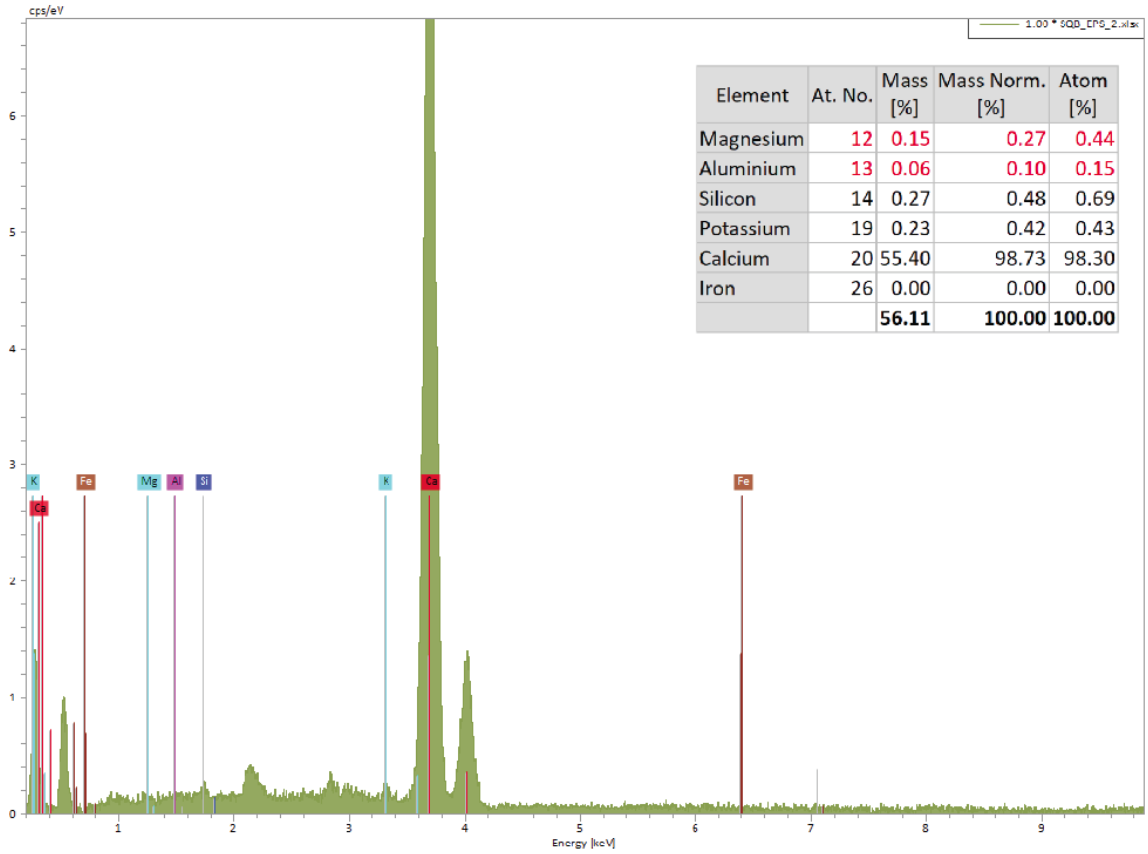


| Element | At. No. | Mass [%] | Mass Norm. [%] | Atom [%] |
|---|---|---|---|---|
| Magnesium | 12 | 0.15 | 0.27 | 0.44 |
| Aluminium | 13 | 0.06 | 0.10 | 0.15 |
| Silicon | 14 | 0.27 | 0.48 | 0.69 |
| Potassium | 19 | 0.23 | 0.42 | 0.43 |
| Calcium | 20 | 55.40 | 98.73 | 98.30 |
| Iron | 26 | 0.00 | 0.00 | 0.00 |
| | | **56.11** | **100.00** | **100.00** |

Figure A13: EDS spectra for point 2 (calcite crystal) seen in Fig. A10. Elemental composition of the analyzed point shows normalized mass of 98.73% calcium (Ca), 0.48% silicon (Si), 0.42% potassium (K), 0.27% magnesium (Mg), 0.10% aluminium (Al), and 0.00% iron (Fe).

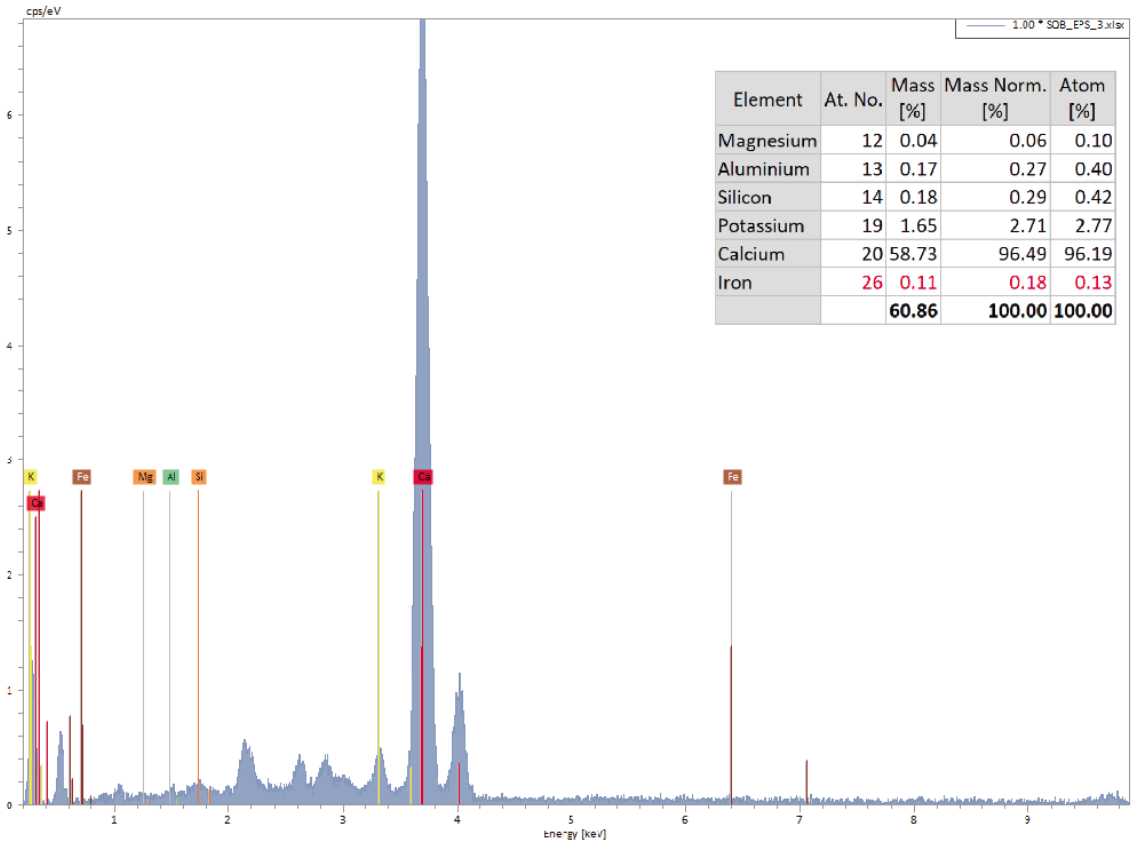


| Element | At. No. | Mass [%] | Mass Norm. [%] | Atom [%] |
|---|---|---|---|---|
| Magnesium | 12 | 0.04 | 0.06 | 0.10 |
| Aluminium | 13 | 0.17 | 0.27 | 0.40 |
| Silicon | 14 | 0.18 | 0.29 | 0.42 |
| Potassium | 19 | 1.65 | 2.71 | 2.77 |
| Calcium | 20 | 58.73 | 96.49 | 96.19 |
| Iron | 26 | 0.11 | 0.18 | 0.13 |
| | | **60.86** | **100.00** | **100.00** |

Figure A14: EDS spectra for point 3 (calcite crystal) seen in Fig. A10. Elemental composition of the analyzed point shows normalized mass of 96.49% calcium (Ca), 2.71% potassium (K), 0.29% silicon (Si), 0.27% aluminium (Al), 0.18% iron (Fe), and 0.06% magnesium (Mg).

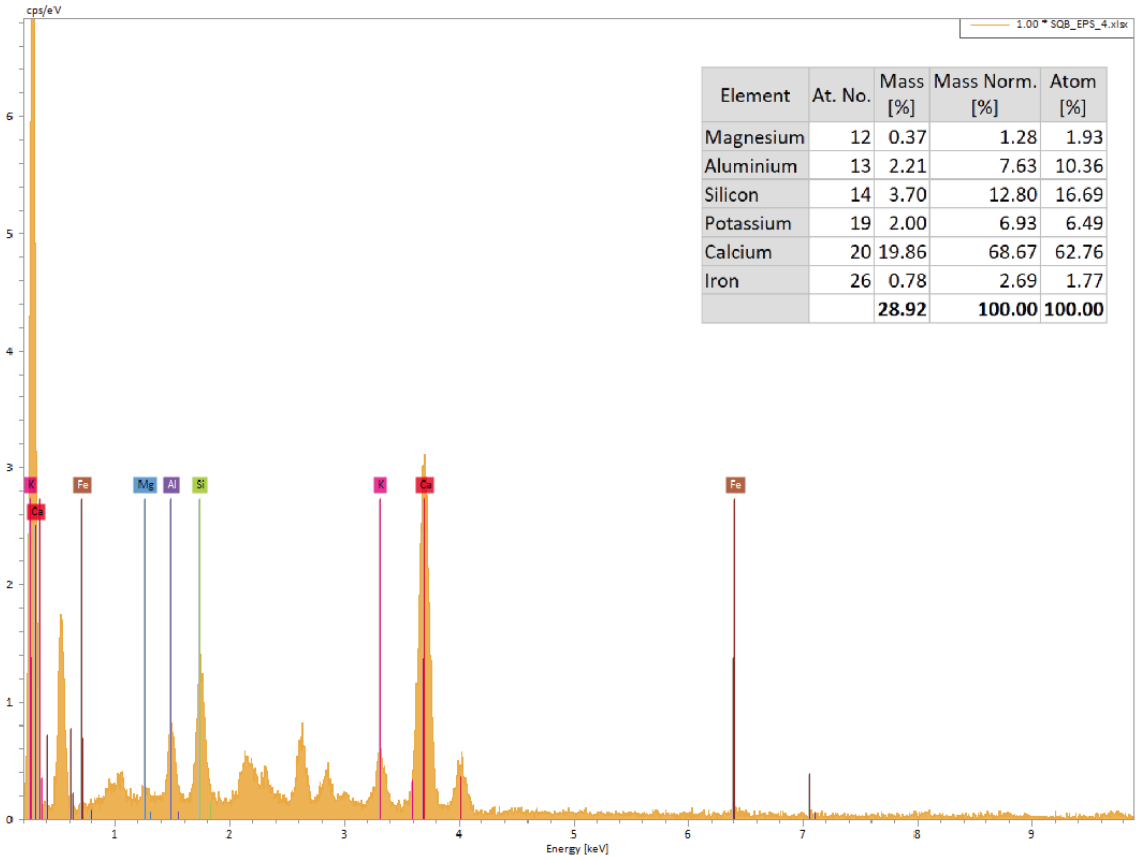


| Element | At. No. | Mass [%] | Mass Norm. [%] | Atom [%] |
|---|---|---|---|---|
| Magnesium | 12 | 0.37 | 1.28 | 1.93 |
| Aluminium | 13 | 2.21 | 7.63 | 10.36 |
| Silicon | 14 | 3.70 | 12.80 | 16.69 |
| Potassium | 19 | 2.00 | 6.93 | 6.49 |
| Calcium | 20 | 19.86 | 68.67 | 62.76 |
| Iron | 26 | 0.78 | 2.69 | 1.77 |
| | | **28.92** | **100.00** | **100.00** |

Figure A15: EDS spectra for point 4 (pore surface) seen in Fig. A10. Elemental composition of the analyzed point shows normalized mass of 68.67% calcium (Ca), 12.80% silicon (Si), 7.63% aluminium (Al), 6.93% potassium (K), 2.69% iron (Fe), and 1.28% magnesium (Mg).

VITA

Alejandra Santiago Torres

Candidate for the Degree of

Master of Science

Thesis: SIGNIFICANCE OF MICROBIAL BINDING IN THE FORMATION AND STABILIZATION OF CARBONATE FOREREEF SLOPE DEPOSITS

Major Field: Geology

Biographical:

Education:

Completed the requirements for the Master of Science in Geology
Oklahoma State University, Stillwater, Oklahoma in July 2019.

Completed the requirements for the Bachelor of Science in Geology the
University of Puerto Rico at Mayagüez, Mayagüez, Puerto Rico in 2017.

Experience:
Geoscience Intern at ExxonMobil Corporation, Houston TX- Summer 2018

Professional Memberships:
American Association of Petroleum Geologists
Society for Sedimentary Geology
Association for Women Geoscientists